

THESIS

A PROBABILISTIC ECONOMIC AND ENVIRONMENTAL IMPACT ASSESSMENT OF A
CYANOBACTERIA-BASED BIOREFINERY

Submitted by

Audrey Beattie

Department of Mechanical Engineering

In partial fulfillment of the requirements

For the Degree of Master of Science

Colorado State University

Fort Collins, Colorado

Summer 2021

Master's Committee:

Advisor: Jason C. Quinn

Mazdak Arabi

Anthony Marchese

Copyright by Audrey Beattie 2021

All Rights Reserved

ABSTRACT

A PROBABILISTIC ECONOMIC AND ENVIRONMENTAL IMPACT ASSESSMENT OF A CYANOBACTERIA-BASED BIOREFINERY

Microbial based biofuels represent a potential promising solution as an environmentally favorable transportation fuel. Cyanobacteria have many of the same advantages as microalgae: ability for rapid growth in otherwise non-arable regions, suitability for genetic engineering, and simple nutritional needs. Additionally, cyanobacteria can be engineered to secrete valuable co-products that can be harvested independent from the produced biomass. However, little work has been done to identify the processes and the economic and environmental impacts associated with a large-scale cyanobacteria-to-fuels facility. The present study is a concurrent techno-economic and life cycle assessment of a facility that generates fuels and methyl laurate, an oleochemical, from the cyanobacterial species *Synechocystis* sp. PCC 6803. The biorefinery model includes all aspects of cultivation, separation of the secreted methyl laurate, biomass harvesting and fuel processing via hydrothermal liquefaction (HTL) of the dewatered biomass. The assessments leverage Monte Carlo analysis (MCA) to address uncertainty and variability inherent in the most significant input parameters, replacing them with probabilistic functions. For the facility configuration producing both fuels and the oleochemical co-product, the MCA average minimum fuel selling price (MFSP) is \$2.47 per liter or \$9.34 per gallon of gasoline equivalent (gge) with the corresponding average global warming potential determined to be 118 g CO₂-eq-MJ⁻¹. The case producing only fuels results in an MCA average MFSP of \$2.01-L⁻¹ (\$7.60-gge⁻¹) and an average environmental impact of 100 g CO₂-eq-MJ⁻¹. These results are compared to static

optimistic and conservative scenario analysis estimates, illustrating the over- and under-estimation of outcomes associated with non-stochastic methods. Suggested facility improvements include increases in pond productivity of both the biomass and methyl laurate oil production, as well as improvements to carbon utilization and bio-crude yield from HTL processing.

ACKNOWLEDGEMENTS

First, I would like to thank my advisor, Jason C. Quinn for his invaluable guidance, support, and patience throughout the course of this work. My thanks also to the other members of my committee, Mazdak Arabi and Anthony Marchese, for their time and support. I am thankful to my collaborators at Arizona State University: Wim Vermaas, Steven C. Holland, Shuqin Li, John McGowen, and David Nielsen, and to Al Darzins at Nano Gas Technologies, for their contributions of data, editing of the manuscript, and advice throughout the project. This work was also supported by members of the Quinn research group: thank you to Jonah Greene, Katie DeRose, and Peter Chen for their contributions to the process modeling that forms the basis of this work, and to Evan Sproul and Hailey Summers for their insights on the life cycle assessment methods. My many thanks to those listed and all the other members of the Quinn group for making my time at CSU both fun and rewarding. Finally, I am incredibly grateful for the support of my parents, siblings, friends, and mentors – I surely would not be presenting this thesis if it weren't for all of you.

This work was supported financially by the United States Department of Energy (DE-EE0008515).

TABLE OF CONTENTS

ABSTRACT.....	ii
ACKNOWLEDGEMENTS	iv
INTRODUCTION	1
METHODS	6
1. Process Modeling.....	6
1.1 Cultivation	6
1.2 Methyl Laurate Harvest	8
1.3 Biomass Dewatering.....	8
1.4 Hydrothermal Liquefaction Conversion.....	9
1.5 Storage	10
2. Techno-economic Analysis.....	10
2.1 CAPEX.....	11
2.2 Variable OPEX	12
2.3 Fixed OPEX.....	13
3. Life Cycle Assessment.....	13
4. Monte Carlo Analysis	15
4.1 Parameter selection.....	16
4.2 Input distribution selection	16
4.3 @RISK Software	18
RESULTS AND DISCUSSION.....	19
1. Baseline Results	19
2. Sensitivity Analysis Results.....	24
3. Techno-economic Analysis Results	29
3.1 Fuels case.....	31
3.2 Fuels and co-product case.....	34
4. Life Cycle Assessment Results.....	37
4.1 Fuels case.....	39
4.2 Fuels and co-product case.....	42

5. Discussion of MCA methodology	45
CONCLUSIONS.....	48
REFERENCES	49
APPENDIX A: SUPPLEMENTARY INFORMATION.....	57

INTRODUCTION

Climate change is largely driven by the emission of greenhouse gases (GHGs), a primary source of which is the combustion of fossil fuel-derived diesel and gasoline for transportation [1]. Biofuels are an alternative fuel that can be directly substituted for fossil fuels with a potentially smaller environmental impact [2], [3]. Algae take up carbon dioxide (CO₂) during growth and can be converted into biofuels and other valuable bio-products after the biomass is harvested and separated from the water. The resulting fuel, converted to a renewable diesel [4]–[6], can be directly substituted for petroleum-derived diesel. Other products include bio-plastics and nutraceuticals, which can be produced concurrently and have higher market values that offset the large production process costs [7], [8]. The vast majority of microalgal biofuel studies have been performed using autotrophic microalgae species. Microalgae are particularly useful organisms for biofuel production because they are often amenable to genetic manipulation, and many display high growth rates [9]. Further, they are able to grow in otherwise non-arable areas and therefore do not compete for land with food agriculture [10]. Cyanobacteria, a group of photosynthetic microbes, represent an emerging area of microbial fuel research. Species from genera such as *Synechocystis* and *Synechococcus* offer many of the same benefits as microalgae, including rapid growth and simple nutrient demands, and are particularly suitable for introducing genetic mutations for improved CO₂ utilization and production of desired compounds [9], [11], [12]. Cyanobacteria are further distinguished from microalgae as some can be genetically engineered to secrete valuable products [13] which can reduce the need for energy-intensive product harvesting techniques.

While microalgal and cyanobacterial biofuels have been physically demonstrated at small scales, the feasibility and impacts of large scale, commercial implementation have yet to be

demonstrated. Sustainability modeling, namely techno-economic analysis (TEA) and life cycle assessments (LCA), have been leveraged to evaluate the respective economic and environmental impacts of an industrial-scale process [14]. These analyses are predicated on a process model that captures the energetic and mass flows through the system and have been implemented with microalgae species in over 60 studies, on a wide range of growth architectures, conversion methods, and bio-products [14]. Some studies focus on the algal growth and dewatering processes alone with the objective of selling the biomass product [15]–[18]. Others consider the conversion process only, purchasing dewatered biomass product and selling a biofuel product [19]–[21] or another bio-product, such as plastics [8]. Finally, many, including the present study, consider the entire pathway, from algal growth through conversion [6], [22]. Compared to that of microalgae, the scientific literature is severely lacking in cyanobacteria-specific TEA and LCA, despite them being widely identified as a promising fourth generation biofuel [12]. Johnson et al. studied the economic impacts of using *Anabaena* sp. PCC 7120 for production of limonene, a biodiesel, followed by anaerobic digestion of the remaining biomass material, reporting facility net present values of -\$558 and \$392 million for a scenario with experimentally demonstrated productivity, and one with improved, “best case” productivity, respectively [23]. Markham et al. performed a TEA on ethylene produced from a recombinant *Synechocystis* sp. PCC 6803, using photobioreactor growth structures and fractionation of hydrocarbons to produce fuel blend stocks, reporting a baseline minimum fuel selling price (MFSP) projection of \$15.07-gge⁻¹ and respective conservative and optimistic projections of \$28.66 and \$5.36-gge⁻¹ [24]. Environmental impacts of cyanobacterial biofuel systems have been studied within a similar scope. Quiroz-Arita et al. assessed the production of three biofuels from *Synechocystis* sp. PCC 6803, attributing the lowest impacts to cyanobacteria-produced ethanol with results between 89.6 and 233.5 g CO₂-

eq-MJ⁻¹ [25]. Nilsson et al. studied a small-scale, 1- ha biorefinery with various growth structures and productivities, finding the GHG emissions associated with the secreted *n*-butanol product from engineered cyanobacteria to be between 16.9 and 58.5 g CO₂-eq-MJ⁻¹, for a range of growth structures and productivities [26]. While these are some of the lowest footprints among cyanobacteria-to-fuels LCA literature, it is extremely unlikely that the modeled location – northern Sweden – would have high enough productivity rates for a commercial facility. Finally, Smetana et al. performed an LCA for the cyanobacterial species *Arthrospira platensis* and the microalgal species *Chlorella vulgaris*, generating a variety of products via three modeled pathways and comparing their environmental impacts [27]. However, these impacts were presented with unconventional units (relative to the annual impact of one European citizen), and therefore make any comparisons to this work very difficult. There are presently no studies with both TEA and LCA on the cyanobacterial strain presented here (*Synechocystis* sp. PCC 6803), nor any that address the conversion of the remaining biomass via hydrothermal liquefaction (HTL), a promising and prominent conversion pathway for wet feedstocks.

The estimation of facility impacts relies on defining the wide range of input parameters related to not only the underlying process but also the economic and environmental characteristics. Ultimately, the quality of TEA and LCA depends on the chosen input parameters, which are often variable and uncertain. Traditionally, TEA and LCA studies have addressed this by reporting conservative, baseline, and optimistic results that are related to a range of inputs in the same categories [24], [28], [29]. While this approach reports a range of possible economic and environmental outcomes, there is no evidence suggesting which of those outcomes are most likely. Monte Carlo analysis (MCA) offers a method for applying stochastic probability to previously static models, thereby giving insight to both the full range of possible outcomes and

how likely they are to occur [30]–[32]. The results from MCA allow for more specific inferences to be made, such as the probability of a certain MFSP being met, or of an environmental burden threshold being exceeded. MCA has been applied in a variety of biofuel studies, across a range of inputs [28], [31]–[39]. Pérez-López et al. performed a well-documented MCA, based on experimental data for three microalgal strains, with probability distributions for a wide variety of input parameters related to the process model as well as economic and life cycle data [32]. Despite its value to sustainability practitioners, there are currently no cyanobacterial biofuel studies that incorporate MCA. Johnson et al. [23] mention probabilistic considerations, but do not describe any MCA methods, nor do they offer details about input or output stochastic distributions.

In general, cyanobacteria-based fuels have been largely under-investigated, with either TEA or LCA being performed on only a select few species or strains and limited downstream processing pathways. Based on the state of the field, there is a need for concurrent TEA and LCA of a cyanobacteria-to-fuels facility with secreted products as well as those converted from the biomass. This work presents an engineering process model of a cyanobacteria-to-biofuel process validated with experimental performance data leveraged for comprehensive TEA and LCA. The modeled strain is *Synechocystis* sp. PCC 6803, which has been engineered to produce methyl laurate, a fatty acid methyl ester that can be used as either a drop-in biodiesel or an oleochemical. As a biodiesel, the methyl laurate has very similar physical properties to diesel from petroleum and can generally be substituted directly in diesel engines. As an oleochemical, methyl laurate can be used in a very wide variety of applications including pharmaceutical, manufacturing, and as a food additive, solvent, or pesticide [40]. This work is among the first cyanobacteria-specific combined TEA and LCA studies (the only for *Synechocystis*), and the

first to model the HTL conversion of cyanobacterial biomass. Further, it is the first that employs MCA and statistical methodology to address inherent variability and uncertainty of input parameters. These results are directly compared to the more typical, non-stochastic scenario analysis results, which estimate the baseline, optimistic and conservative scenarios. This work evaluates the accuracy of static scenario analysis and offers recommendations for addressing variability and uncertainty in future biorefinery studies.

METHODS

1. Process Modeling

The basis of this work is a foundational process model, which captures all mass and energy flows through the system. The system has two product configurations – in the first, the methyl laurate is sold as renewable diesel and assumed to have the same selling price as the biofuel produced from the conversion of biomass via HTL. In the second configuration, the methyl laurate is sold as an oleochemical co-product, and the only fuels sold from the system are generated from the biomass. These configurations are referred to as “fuels” and “fuels and co-product,” respectively. The system boundary is shown in Figure 1, with required mass and energy inputs for the various sub-processes.

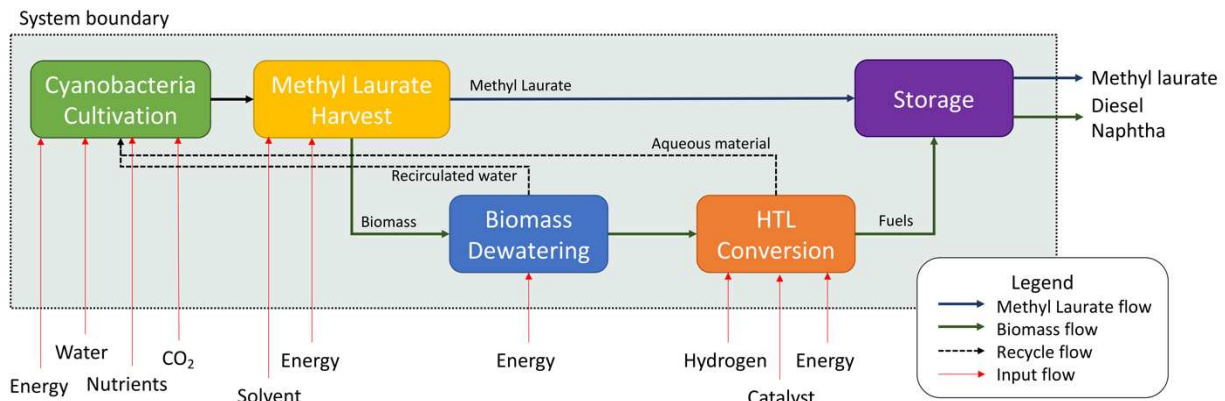


Figure 1: The system boundary illustrates the processes and inputs captured by the process model, broken down into process modules. The mass flows for the methyl laurate and biomass are illustrated with blue and green lines, respectively.

1.1 Cultivation

The cultivation module was modeled closely after the process report of Davis et al., with a two-stage inoculation system before the full-size ponds [15]. Due to the genetic engineering of the cyanobacteria, the growth ponds were assumed to be covered. The total area of the ponds was

2,023 hectares (5,000 acres), and the areal productivity was assumed to range from 12 to 15 g-m²-day⁻¹, based on experimental data from outdoor growth trials. The secreted methyl laurate was assumed to be produced as a ratio of the biomass productivity, ranging from 0.25 to 0.50 g-g⁻¹, also based on experimental data. The nutrient demands for the system were met by a cyanobacteria-specific growth medium (PE-001A), an inexpensive mix that mimics BG-11 [41]. The nutrient needs of the ponds were calculated according to the stoichiometric compositions of the cyanobacterial biomass and the growth medium. Monoethanolamine, an amino alcohol that assists with CO₂ uptake, was added to the ponds with the nutrient mix at a concentration of 0.2 mM. Energetic inputs to the ponds included mixing by a paddlewheel that required 77.1 kWh-ha⁻¹-day⁻¹.

In addition to the ponds, the cultivation module included the CO₂ delivery system: a five-foot deep sump sparging system. The CO₂ requirements were found in a similar way to nutrient requirements, with the carbon content of the cyanobacteria and the off-gassing rate of the sparging system. The carbon content of the biomass and methyl laurate product was assumed to be 51.4%, and 73%, respectively. The CO₂ utilization rate of the system ranged between 20% and 40%, with an average of 33% [32], [42]. The sump was calculated to use 46 kJ of electricity per kg of CO₂ gas to overcome the five-foot depth, and another 36.1 kJ per kg for fans and blowers used throughout the facility [42]. The delivered CO₂ was assumed to be nearly pure (between 97.5% and 100%), sourced from one of a variety of industries detailed by Last and Schmick [43]. The biorefinery facility was assumed to be co-located with a facility for one of these industries, so no extra transportation of the CO₂ was included.

1.2 Methyl Laurate Harvest

The system was operated in a semi-continuous mode with 20% of the pond being harvested every day, which corresponds to a volumetric flowrate of 404,600 m³ per day. The harvested material was processed through a novel oil separation process before the biomass was sent to the dewatering module. First, a dodecane solvent was mixed into the harvested volume in an agitation tank, separating the methyl laurate from the biomass by partitioning the methyl laurate in the dodecane phase. Then, the lighter dodecane-methyl laurate solution was separated from the heavier biomass material by a series of coalescence plates. The energy requirements of the agitation tank were estimated to be between 0.04 and 0.1 kW per m³ of throughput [44]. The coalescence plates, similar to settlers used for dewatering, were passive and did not require energy. The combination of the mixing tank and settling plates is referred to as the mixer-settler. After separation, the dodecane-methyl laurate mixture was sent to a distillation column to recover the methyl laurate to an assumed purity of 99%. The methyl laurate was stored as either a drop-in biodiesel or an oleochemical, depending on the facility configuration. The dodecane was recycled within the methyl laurate harvest process with a 99.5% recovery rate. The distillation column was modeled in Aspen and estimated to require approximately 1524 kJ of heating energy or 0.04 scm (1.4 scf) of natural gas per kg of solution throughput.

1.3 Biomass Dewatering

The biomass dewatering process for the produced biomass consisted of three stages: a settler followed by a membrane and then a centrifuge. The settler was assumed to bring the biomass from 0.07% solids to 1% solids. The membrane achieved 13% solids, and finally the centrifuge brought the volume to 20% solids. The dewatering systems required 0, 0.04 and 1.35 kWh per cubic meter of throughput for the three stages, respectively [15]. As a whole, the

dewatering process retained 86% of the biomass, the balance remaining in the clarified water. The clarified water was recirculated back to the main ponds for recycling. In all, the system retained 99.5% of the biomass [15].

1.4 Hydrothermal Liquefaction Conversion

The modeled system used HTL followed by hydro-treatment to convert the dewatered biomass to fuel products. The HTL and upgrading module was modeled closely after that of the Jones et al. process report [19]. The dewatered biomass was pumped through a preheating system and then an HTL plug flow reactor. The resulting products were divided by a filter and three-phase separator into char, aqueous material, and bio-crude. The bio-crude continued to a hydro-treating and hydrocracking process, where it was pumped through a series of columns and a heater to separate the crude oil into naphtha, diesel, and off-gasses. Meanwhile, the solid char was sold for the price of removal from the facility. The aqueous material was cooled and returned to the ponds for the purpose of recycling nutrients. This is assumed to be a seamless integration [19], [45]. The naphtha and diesel were taken to be stored and the off-gasses were processed in an ammonia scrubber. The input flowrate to the HTL system was approximately 17 kg of dewatered biomass per second, although this varied slightly based on the productivity of the pond. The volume of fuels produced from HTL is governed by bio-crude yield, which ranged from 30% to 60%, with an average of 40%. For a bio-crude yield of 45%, the combined total energy usage of the conversion module was approximately 1,740 kJ per kg ash-free dry weight (AFDW) algae throughput, approximately 88.5% of that being heat supplied by natural gas, and the balance supplied by electricity.

1.5 Storage

The biofuel products are stored in tanks sized for 24 hours of production, consistent with the process design of Davis et al. [15]. There was a separate tank for each product: methyl laurate, diesel and naphtha. Additionally, there are tanks to store make-up water, approximately 3,324 m³ (878,000 gallons).

2. Techno-economic Analysis

TEA involves superimposing economic and financial data on the process model data, resulting in an estimation of MFSP for the system based on economic assumptions. There are three primary types of costs: capital expenses (CAPEX), operational expenses (OPEX) and fixed OPEX, such as labor. These expenses are accounted for in a discounted cash flow rate of return (DCFROR), which undergoes an iterative solving process to find the fuel selling price at which the net present value of the system is zero. This selling price is the minimum volumetric price at which the facility will achieve the fixed internal rate of return over the lifetime of 30 years. The DCFROR and TEA employed the Nth of a kind (NOAK) economic assumptions, as outlined in Table 1.

Table 1: "Nth of a kind" economic assumptions [46]. All are standard except operation days, which have been included as a variable input parameter.

Parameter	Standard value
Internal rate of return	10%
Facility debt / equity	60% / 40% total capital
Facility lifetime	30 years
Income tax rate	35%
Interest rate	8% annually
Debt financing term	10 years
Working capital	5% fixed capital (excluding land)
Depreciation schedule	7-year modified accelerated cost recovery system
Construction period	8% year 1

	60% year 2
	32% year 3
Plant salvage value	None
Start-up time	6 months
Start-up revenue and costs	50% revenue
	75% variable costs
	100% fixed costs
Indirect capital	60% total installed capital
Base cost year	2018

2.1 CAPEX

The majority of the CAPEX estimation for the cultivation, dewatering and storage systems followed the process modeling of Davis et al. [15]. Likewise, the HTL and upgrading conversion system costs were modeled after that of Jones et al. [19]. However, the current system had different volumetric throughput and corresponding size requirements from the source literature. Capital costs were found using Equation 1, and brought to 2018 dollars using cost indices:

$$Scaled\ CAPEX = Source\ CAPEX \left(\frac{Scaled\ throughput}{Source\ throughput} \right)^n \quad \text{Eqn. 1}$$

Here, n is a scaling factor, which varies for each piece of equipment or system. Information about specific scaling factors can be found in the work of Davis et al. [15] and Jones et al. [19].

The harvest module CAPEX was estimated from Brown [47], with the mixer-settler tank being priced separately, as well as the distillation columns. The mixer-settler consisted of an agitator and a tank sized on the volumetric throughput of the biomass-solvent solution, according to Equations 2a through 2c [47]:

$$Mixer\ (\$K) = 3.14(HP)^{0.40} + 3.33(HP)^{0.77} \quad \text{Eqn. 2a}$$

$$Tank\ (\$K) = 0.8V^{0.83} \quad \text{Eqn. 2b}$$

$$\text{Mixer settler } (\$K) = 1.5(\text{Mixer} + \text{Tank}) \quad \text{Eqn. 2c}$$

Here, HP refers to the required horsepower, which is calculated from the mixer-settler energy requirement multiplied by the throughput. In equation 2b, V is the volumetric capacity of the tank. In equation 2c, 1.5 is the install factor, which is the additional cost required for installation of the equipment [19].

The distillation column purchase and installed costs were found similarly, calculated according to a pressure vessel cost estimation [47]:

$$PV (\$K) = 5.18V^{0.67} \quad \text{Eqn. 3a}$$

$$\text{Distillation column } (\$K) = 1.7(1.5PV) \quad \text{Eqn. 3b}$$

PV is the capital cost of the pressure vessel, V refers to the volumetric capacity of the column, and the install factor is 1.7 [19].

All costs were brought to 2018 dollars using the following equation with the relevant cost indices [14]:

$$\text{Cost in 2018\$} = \text{Original cost} \left(\frac{\text{2018 Index}}{\text{Original Year Index}} \right) \quad \text{Eqn. 4}$$

2.2 Variable OPEX

Variable operational costs for the system include consumables, such as nutrient requirements and CO₂, and chemical additives such as the solvent used in the harvest module and the hydrogen used for the hydro-treatment following HTL. It also includes all electricity and natural gas costs. Similar to CAPEX, much of the OPEX was scaled from source literature, particularly Davis et al. [15] and Jones et al. [19], according to Equation 5:

$$\text{Scaled OPEX} = \text{Source OPEX} \left(\frac{\text{Scaled throughput}}{\text{Source throughput}} \right) \quad \text{Eqn. 5}$$

2.3 Fixed OPEX

Fixed operational expenses are costs of the system that are not subject to changes in volumetric throughput, such as labor and maintenance. Facility labor includes plant managers, engineers, supervisors, and technicians. Facility maintenance was calculated as 3% of the harvest and dewatering CAPEX and 0.5% of the other module CAPEXs. Facility labor requirements were found according to the reports from Davis et al. [15] and Jones et al. [19], scaled, and brought to 2018 dollars. Both upstream and downstream portions of the facility required plant managers, engineers, laboratory technicians and managers, yard employees, and clerks and secretaries. The number of roles required for the upstream portions of the plant were scaled on facility area, and downstream labor was scaled on volumetric throughput, according to Equations 6a and 6b.

$$\text{Upstream labor} = \text{Source quantity} \left(\frac{\text{Facility footprint}}{\text{Source footprint}} \right) * \text{Salary} \quad \text{Eqn. 6a}$$

$$\text{Downstream labor} = \text{Source quantity} \left(\frac{\text{Facility throughput}}{\text{Source throughput}} \right) * \text{Salary} \quad \text{Eqn. 6b}$$

An additional labor burden accounted for overhead costs associated with facility employees and was assumed to be 90% of the total calculated labor costs, based on the process models from Davis et al. [20] and Jones et al. [19].

3. Life Cycle Assessment

An LCA was conducted by overlaying life cycle inventory data on the foundational process model and was used to find the environmental burdens of the process. Life cycle inventory data were accessed using OpenLCA and the ecoinvent v3.4 database [48]. The life cycle information (LCI) considered was global warming potential (GWP), quantified through

aggregating GHGs. The GHGs were found for each individual consumable, usually per kg for mass inputs and in base energetic units for others. The LCIs were determined for all of the consumables, electricity, and natural gas used throughout the facility via ecoinvent v3.4. Where possible, all LCIs were pulled for cutoff, system processes, which means the processes to create the consumable are fully aggregated, and their end use emissions are not assumed. These characteristics were then accounted for across the consumables used in the facility and normalized on the basis of fuel energy produced by the system, according to the TRACI v2.1 methodology [49].

For the fuels case, impacts across the facility were summed and allocated equally per MJ of fuel energy as the scenario is limited to producing fuels. In the fuels and co-product case, the impacts were allocated based on relevant sub-process modules and economic allocation where division based on process is not possible. This approach is consistent with the ISO 14044:2006 standard [50]. The portion of the facility dedicated only to the biomass-to-fuels pathway (dewatering through conversion) was separated from the portion that deals with the methyl laurate product. Those emissions were then attributed directly to the produced fuels. The cultivation and harvest modules dealt with both the methyl laurate and biomass, and thus those impacts were allocated based on the economic value of the two products, according to Equation 7:

$$E_{F,total} = (-C_U + E_{100} + E_{200} + E_{600}) \left(\frac{V_F m_F}{V_{ML} m_{ML} + V_F m_F} \right) + E_{300} + E_{400} \quad \text{Eqn. 7}$$

Here, $E_{F,total}$ is the total GHG emissions attributed to the fuels, brought to their 100-year CO₂ equivalents. C_U is the CO₂ taken up by the ponds, and E_{100} , E_{200} and E_{600} are the CO₂ equivalent emissions from the respective growth, harvest and storage modules that are shared by the biomass and methyl laurate. V_F and V_{ML} are the respective volumes of fuel and methyl

laurate, and m_F and m_{ML} are the respective market values of those products. E_{300} and E_{400} are the CO₂ equivalent emissions from the remaining modules, dewatering and conversion, that are totally allocated to the fuels. A more detailed breakdown of the system boundaries inherent in this allocation process is shown in the supplementary information (Figure A1), as well as impacts resulting from the mass allocation method (Table A1). Because the oleochemical can be used for a wide variety of applications, the system boundary for this analysis ends at the delivery of the product. Thus, combustion of the methyl laurate was not considered in the co-product configuration. Results are presented per MJ of fuel energy, to maintain consistency between results and to allow for comparison with the renewable fuel standard and other fuel studies.

4. Monte Carlo Analysis

MCA replaces static input parameters with probabilistic distributions, which more adequately captures the inherent uncertainty in the model and allows for a greater resolution of the model outcomes. To start, uncertain and variable parameters were identified and replaced with probabilistic functions. For this work, these parameters were chosen based on their relative impact on the model results which was determined through sensitivity analysis. Then, their representative input distributions were defined, informed by literature survey and experimental data. The chosen input distributions are described in more detail in section 4.1 and can be found for specific parameters in Tables A2, A3 and A4 of the supplementary information. Finally, the model was simulated with a random sampling of inputs from their respective distributions for 5000 iterations. This was deemed sufficient by comparison to results of runs with 10,000 iterations – the differences in output summary statistics were negligible. Results of this analysis are shown in Figure A2 and Tables A5 and A6 of the supplementary information.

4.1 *Parameter selection*

Parameters that were replaced with probabilistic functions were chosen based on the system-wide sensitivity analysis. The sensitivity analysis was performed by varying each input individually, and finding which parameters were linked to the greatest overall change [30]. This is a local sensitivity analysis method, also known as “one-[factor]-at-a-time,” which focuses on the influence of individual parameters on the system, and not necessarily on the influence of interactions between parameters [30]. Each parameter was varied by $\pm 50\%$ and the resulting MFSP and GWP were recorded on each side. Those with a change in TEA or LCA results greater than or equal to 5% were considered significant enough to be included in the MCA. In a likewise analysis to iteration number, results with a selection criterion of 5% or greater relative impact were compared to that of 1% or greater impact. The differences in summary statistics were negligible and the 5% selection criterion was deemed sufficient. These results are presented in Figure A3 and Tables A5 and A6 of the supplementary information. This approach is consistent with guidance for performing MCA from the United States Environmental Protection Agency, which advises that variables identified through sensitivity analysis as non-significant may be fixed, although it should be made clear that these parameters are not necessarily considered constant [51]. Parameters in this category likely have some variability or uncertainty, but they may be left out of the scope of MCA due to their insignificant effect on the system outcomes. Further explanation of parameters included in the MCA and their assigned input distributions is given in section 4.2.

4.2 *Input distribution selection*

Once the parameters of interest have been elucidated, the probability distributions for those parameters are selected based on literature or fitted to experimental data. In general,

parameters with little or no data were represented with uniform distributions, which are the least specific and give all values of the range equal probability of occurring. Parameters with source material or adequate data can be represented with more sophisticated probability distributions. Many of the distributions used in the present study were modeled according to experimental or literature data and with shapes similar to Pérez-López et al. [32] including pond productivity, methyl laurate production, CO₂ off-gassing rate and electricity cost. Other parameters were represented by probability distributions that have been fitted to data using the @RISK distribution fitting tool [52]. This was the case for bio-crude yield from HTL, operation days, growth pond CAPEX, and methyl laurate market selling price. Distribution fit was assessed using Akaike information criterion (AIC), Bayesian information criterion (BIC), and Kolmogorov Smirnov (KS) testing [51], [53], [54]. More details regarding the chosen probability distributions are available in Tables A2, A3 and A4 of the supplementary information.

Most of the parameters highlighted by the sensitivity analysis are considered variable – they exist within a known range that is the result of varying assumptions and sources [51], [55], [56]. For example, the CAPEX of the growth ponds is variable, due to a range of estimations that have been given by different contractors. Similarly, bio-crude yield has been shown experimentally to exist within a range between 30% and 60% – it is variable but not uncertain. Thus, these input distributions were fit to data found in the literature. Other parameters, particularly those associated with the first of a kind aspect of the model, are considered uncertain. Uncertain variables are those that have not been studied enough to be prescribed specific values from literature [51], [55], [56]. The only parameter deemed uncertain in this study is the dodecane solvent concentration, used to separate the methyl laurate from the biomass product in the harvest module. The central value for this parameter has been assumed from

experimental data and assigned a uniform distribution with a range $\pm 10\%$ the experimental value.

4.3 *@RISK Software*

The software used to perform the MCA is the @RISK software from Palisade, which operates within the Microsoft Excel framework and is used to execute the iterative MCA process [52]. Upon each iteration, a new value is chosen randomly from the probability distribution for each selected input variable. This produces a set of outputs, such as environmental impact and financial data. For an MCA of n iterations, there are n outputs for each chosen outcome parameter. For the present study, outcomes of interest were MFSP and GWP. The individual outputs were aggregated to determine cumulative output distributions for the two metrics. Additionally, the @RISK distribution fitting tool was used to generate some of the input distributions, as described in section 4.2.

RESULTS AND DISCUSSION

This model considers two cases regarding treatment of the secreted methyl laurate product. In one case, it is treated as a biodiesel product and is included in the volume of fuels sold at the MFSP. In the other case, it is sold as a co-product with a separate, fixed selling price with its own input probability distribution. These cases are referred to as “fuels” and “fuels and co-product,” respectively.

1. Baseline Results

The following figures show the economic (Figure 2) and environmental (Figure 3) impact results for the static baseline scenario. This scenario assumes the average values for all input parameters and is used to illustrate the contributions of the individual unit process operations. In scenarios with negative contributions (i.e., co-product credits, carbon uptake credits), the net impact is denoted with a black diamond.

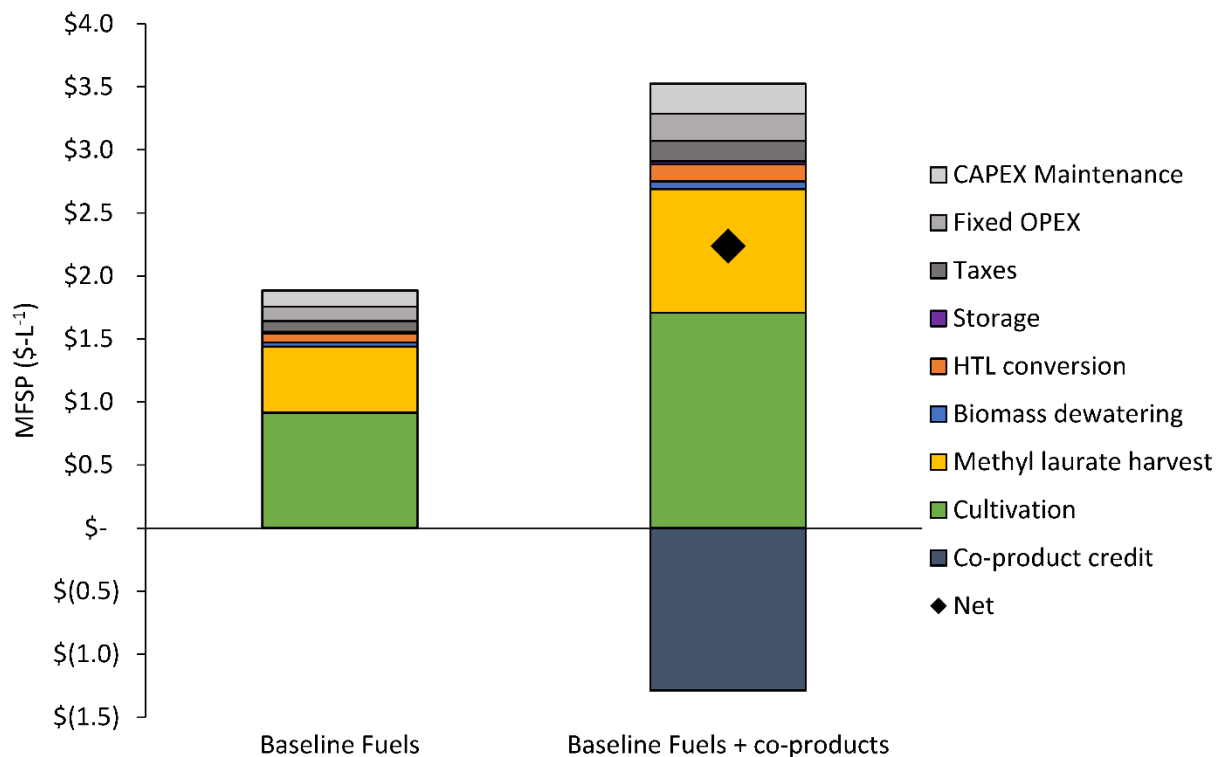


Figure 2: Static baseline economic impact results for the fuels case (left) and fuels + co-products case (right). When there are negatively valued bars, such as for co-product credits, the net result is illustrated with the black diamond. The net results are $\$1.89\text{-L}^{-1}$ ($\$7.14\text{-gge}^{-1}$) for the fuels case and $\$2.24\text{-L}^{-1}$ ($\$8.47\text{-gge}^{-1}$) for the fuels and co-products case.

The growth module takes the largest share of the economic burden, followed by methyl laurate harvest, for both cases. The first is due to the high capital expenses associated with the covered ponds, the energetic demands of the ponds, labor, and nutrient costs. The annual fertilizer cost is approximately 2.5 times greater than the annual cost of energy for pond mixing by paddle wheel and recirculation of water from the dewatering module, and accounts for nearly half of the pond OPEX. Energy used to deliver carbon as CO₂ consumes less than 10% of the cultivation module OPEX. The ponds make up almost 60% of the total cultivation module CAPEX, followed by general construction expenses such as the warehouse and project contingency. Next, the harvest module has very high operational costs due to the electricity consumption of the mixer-settler, which processes the entire volume of methyl laurate, dodecane

solvent, water and biomass. This results in very high operational costs despite similar per-kg energy intensity of processes further downstream. For example, the distillation process separating methyl laurate from the dodecane solvent is almost 200 times more energetically intensive per m³ of throughput but sees 0.1% of the volume that is processed through the mixer-settler. Capitally, the mixer-settler and distillation columns are approximately equal and each account for nearly 30% of the harvest CAPEX. The balance is attributed to other facility expenses, similar to that of the cultivation module.

The large difference in MFSP between the two cases is related to the assumed value of the methyl laurate. The average market value was assumed to be \$1.78-kg⁻¹, which is not enough to achieve parity with the fuels case, nor with conventional fuels benchmarks. To match the baseline fuels case selling price of \$1.89-L⁻¹ (\$7.14-gge⁻¹), the average methyl laurate market value must be at least \$2.26-kg⁻¹, an almost 20% increase. To achieve parity with conventional fuels at \$0.80-L⁻¹ (\$3-gge⁻¹), the methyl laurate market value must be twice the original value, at least \$3.78-kg⁻¹. This assumes an average methyl laurate production ratio of 0.33 g-g⁻¹ of biomass and a biomass productivity of 13.5 g-m⁻²-day⁻¹. Leaving the methyl laurate production ratio the same and increasing biomass productivity to 25 g-m⁻²-day⁻¹, the methyl laurate market value needs only be \$1.92-kg⁻¹ to meet 0.80-L⁻¹ (\$3-gge⁻¹) target. Another contributing factor to this trend is that treating methyl laurate as a co-product decreases the total volume of fuels, so the per-liter costs of individual unit processes increase. While increasing the value of the methyl laurate will increase the size of the co-product credit (the dark blue bar in Figure 2), only an increase in biomass productivity or bio-crude yield will shrink the per-volume costs for each downstream processing module.

The environmental impact results shown in Figure 3 are reported as GWP, on the basis of CO₂ equivalent, which describes the combined GHG emissions from the facility and all processes related to the consumables up until their use in the facility. Grams of CO₂ equivalent (g CO₂-eq) is the 100-year GWP – essentially an accounting of the associated GHG emissions, weighted according to their individual impact relative to CO₂. These emissions are then normalized on the basis of produced fuel energy (MJ) – the volume of fuel multiplied by its energy content. This allows for direct comparison to other fuel sources, such as petroleum-derived diesel or gasoline.

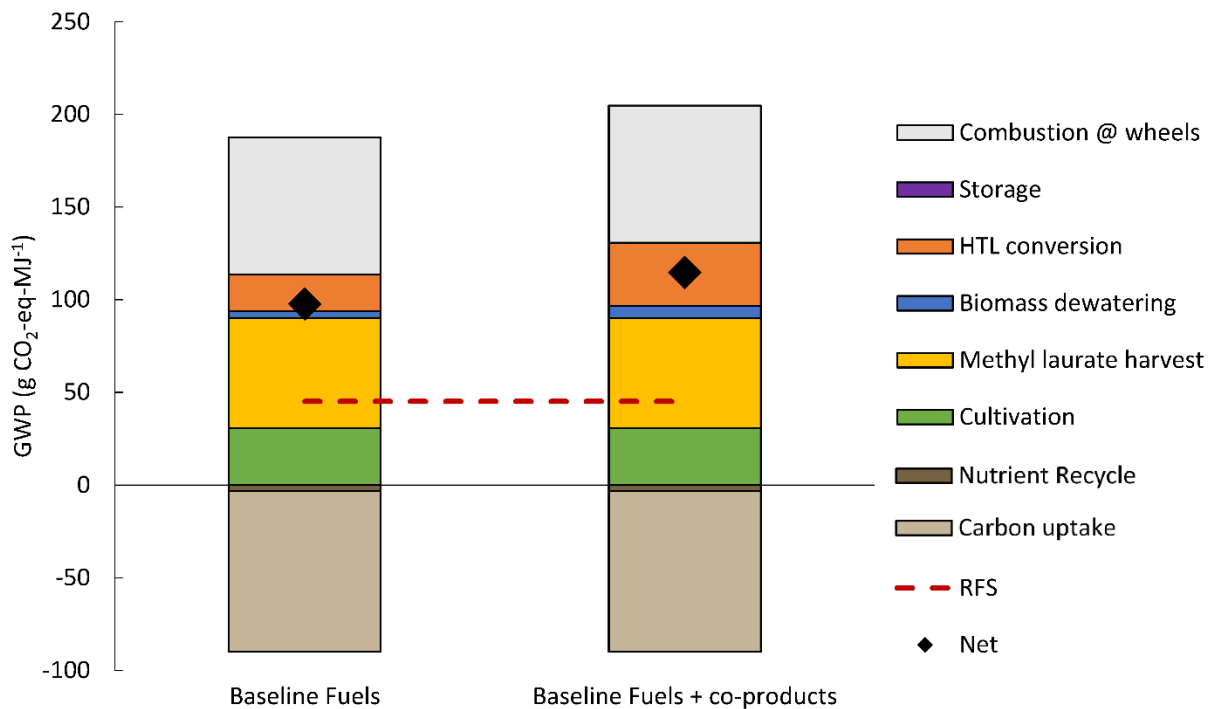


Figure 3: Baseline environmental impact results for the fuels case (left) and fuels and co-products case (right). The net results, illustrated with black diamonds, are 98 g CO₂-eq-MJ⁻¹ and 115 g CO₂-eq-MJ⁻¹, respectively. The renewable fuel standard (RFS) is shown as a red dashed line. In the fuels and co-products case, the baseline methyl laurate impact is 3 g CO₂-eq-MJ⁻¹ (not pictured in the figure).

The static baseline impact of the fuels case is 98 g CO₂-eq-MJ⁻¹, compared to 115 g CO₂-eq-MJ⁻¹ for the fuels and co-product case, shown in Figure 3. The cultivation, harvest, and

conversion modules have the greatest life cycle impact of the facility process modules. However, that combination is nearly matched in magnitude by the carbon uptake credit. Carbon uptake accounts for the amount of CO₂ absorbed in the growth of the cyanobacteria. There is also a modest carbon credit in the nutrients returned to the ponds from the aqueous material leaving the conversion process. The methyl laurate harvest module is very energetically intensive, particularly using heat from natural gas. Additionally, the dodecane solvent used in the harvest module has a large LCI, or footprint prior to reaching the biofuel facility, increasing the impact of this module. The conversion process is also energetically intensive, with much of that being heat delivered by natural gas. However, with less volumetric throughput than the harvest module, its overall impact is much smaller in comparison. Combustion of the fuel is assumed to be another 72 g CO₂-eq-MJ⁻¹ [14] and is attributed to the fuels coming out of the system. This addition completes the well-to-wheels system boundary.

The environmental impact benchmark is the renewable fuel standard (RFS), which is half the GHG emissions of petroleum and is equal to 45 g CO₂-eq-MJ⁻¹ [57]. The baseline results show that the fuels have impacts that are larger than petroleum's 90 g CO₂-eq-MJ⁻¹. This is largely due to high energy demands in both the cultivation and methyl laurate harvest modules for pond mixing, carbon delivery, and distillation separation of the methyl laurate and biomass. Increases in both biomass and methyl laurate productivity can have positive impacts on the environmental footprint of the fuels in both cases. Increasing cyanobacteria pond productivity to 25 g-m⁻²-day⁻¹ decreases the GWP by 36% (62 g CO₂-eq-MJ⁻¹) and 32% (78 g CO₂-eq-MJ⁻¹) in the fuels and fuels and co-products cases, respectively. Adding to that a 50% increase in methyl laurate production ratio to 0.5 g-g⁻¹ brings the GWP down even further to respective impacts of 55 g CO₂-eq-MJ⁻¹ (43% reduction from baseline) and 74 g CO₂-eq-MJ⁻¹ (35% reduction).

Increasing productivity has the most immediate effect for reducing both environmental and economic impact and targeting the respective established benchmarks.

Another important aspect of the LCA results is the allocation of emissions between the two products in the fuels and co-products case. As outlined in the methods, the impacts of the cultivation and harvest modules are allocated based on the relative market value of the two products. As the value of methyl laurate increases, the impacts of the first two modules allocated to the fuel product decreases. The results for both cases are presented as the fuel impacts only, which allows for comparison between the two cases and also among other fuel studies in the field. The baseline methyl laurate impact is 3 g CO₂-eq-MJ⁻¹. This very low impact is credited to two main factors: first, the portions of the facility allocated between the two products include the cultivation module, which has the largest carbon uptake credit. Second, when it is treated as a co-product, the methyl laurate does not incur a combustion impact like the fuels do, which must be included to complete the well-to-wheel system boundary. This further reduces methyl laurate's impact compared to that of the fuel products. The implications of the economic allocation of emissions on the facility impacts are further discussed in section 4.2 of the results and discussion.

2. Sensitivity Analysis Results

A sensitivity analysis was run to determine which parameters were to be included in the MCA and to better understand the system dynamics. This involves varying each parameter \pm 50% individually and recording the relative change in the MFSP and GWP from baseline. The sensitivity results for the system up to 1% impact are shown in Figure 4 and Figure 5.

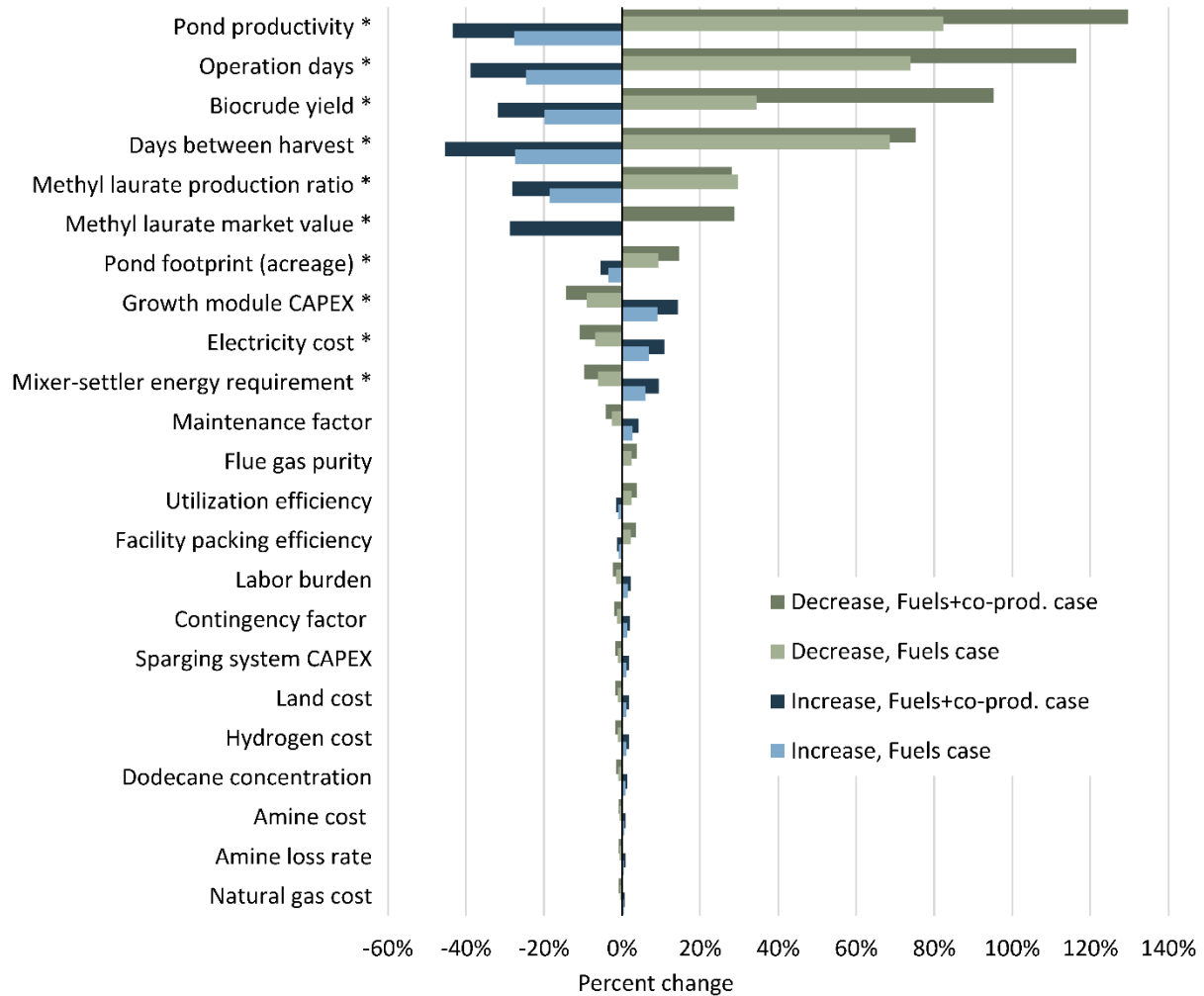


Figure 4: Facility-wide sensitivity assessment on MFSP. The lighter bars correspond to the fuels case, and the darker bars correspond to the fuels and co-product case. Positive green bars mean a decrease in that parameter leads to an increase in MFSP and vice versa. Likewise, positive blue bars mean an increase in that parameter corresponds to an increase in MFSP. Results are included for parameters with impacts greater than or equal to 1%, with those greater than or equal to 5% denoted with an asterisk.

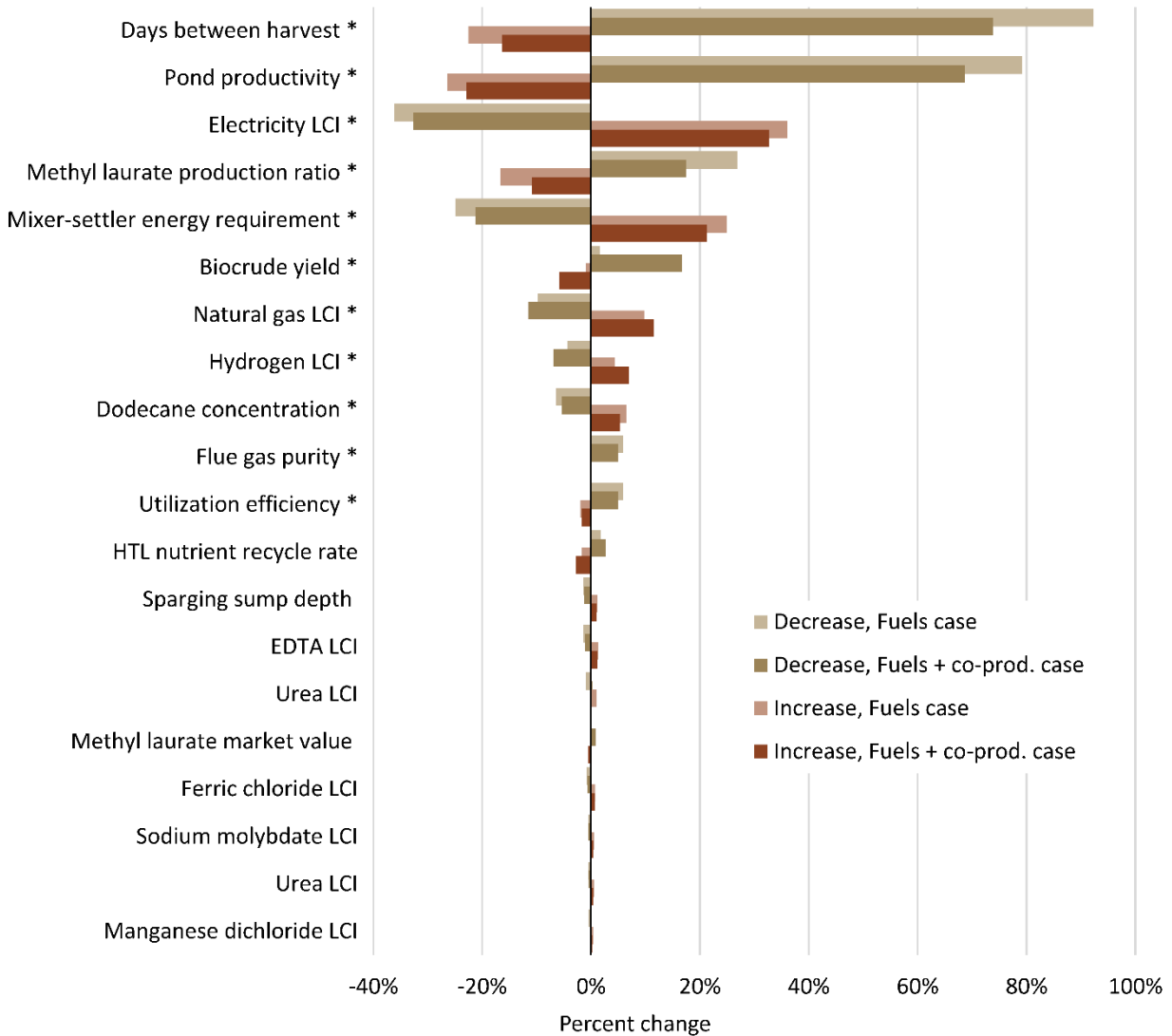


Figure 5: Facility-wide sensitivity assessment on GWP. The lighter bars correspond to the fuels case and the darker bars to the fuels and co-product case. Positive red bars mean a decrease in that parameter leads to an increase in GWP and vice versa. Likewise, positive brown bars mean an increase in that parameter corresponds to an increase in GWP. Results are included for parameters with impacts greater than or equal to 1%, with those greater than or equal to 5% denoted with an asterisk.

The most impactful parameters are process inputs, which are those inputs that are directly related to mass or energy, as opposed to expenses or life cycle inventory characterizations. The largest of these are related to cultivation – pond productivity, operation days, methyl laurate production ratio, CO₂ utilization efficiency, and growth module CAPEX. Productivity (both of the biomass and methyl laurate) and operation days directly affect the amount of biomass, and

therefore fuels, that are generated by the system. Both MFSP and GWP are accounted for per fuel volume, so it is expected that these parameters have such large impacts on both the economic and environmental results. Also related to the cultivation module is CO₂ utilization efficiency, which governs how much of the delivered CO₂ is taken up by the ponds. Importantly, this does not have any bearing on the physical CO₂ emissions from the facility – any off-gassed CO₂ is attributed to the co-located source facility. The biorefinery facility only takes credit for the CO₂ that is taken up, which is dependent on the carbon content of the biomass and therefore constant regardless of utilization efficiency. Utilization efficiency solely affects the volume of CO₂ that must be delivered to the ponds; a decrease in utilization efficiency requires that more CO₂ be delivered, increasing energy requirements, costs, and emissions. The importance of CO₂ utilization has been noted by many, particularly by Somers et al. who evaluated several CO₂ sources and delivery systems and quantified their impact on MFSP and GWP [42].

The most impactful economic input is the market value of methyl laurate, which is present in both the economic and life cycle sensitivities due to the economic allocation method used for calculating GWP. As noted in section 1 of the results and discussion, the market value of methyl laurate has a potent effect on both the MFSP and GWP outcomes, especially when combined with changes in productivity. This effect is further demonstrated by the high positions of pond productivity, methyl laurate production ratio, and methyl laurate market value in the sensitivity analysis. Additional economic parameters include growth module CAPEX and electricity cost. Growth module CAPEX represents the pond construction and installation costs, which are some of the largest CAPEXs in the facility and their range is outlined in Davis et al. [15]. Electricity is one of the most prevalent consumables of the system, so it is expected that its cost is a high-impact variable. The NOAK financial parameters were not varied in this work – it

is already known that those parameters, especially internal rate of return, have very large impacts on the system economics [58]. Since these parameters are clearly defined by the NOAK assumptions, it was deemed unnecessary to investigate their variation or uncertainty.

Another notable category of sensitive parameters is the LCIs associated with the individual consumables used by the system. Life cycle data is inherently variable due to the wide range of assumptions required for calculation and inventory and were included in the sensitivity to establish the influence of this variability on system outcomes. The most impactful shown in Figure 5 are those of electricity, natural gas, and hydrogen. Electricity and natural gas are two of the most widely-used consumables in the facility and hydrogen has a relatively large per-kilogram individual impact. Therefore, it is expected that these are the most impactful of the LCIs.

Of the most impactful parameters identified by the sensitivity analysis, there are two that were not included in the MCA: pond footprint and the number of days between pond harvesting. Pond footprint is the surface area of the biomass ponds and governs the amount of biomass produced as well as land purchased. Days between harvests are related to the semi-continuous pond harvest schedule and directly affect the volume of biomass harvested each day. Decreasing the days between harvest means smaller volumes are collected each day, reducing the energetic and cost demands of the downstream processing systems. Both of these parameters have been left out of the MCA because they are specific to the modeled facility and do not change once they have been chosen. That is, once the facility has been constructed and begins operation, the pond footprint and harvest schedule are not subject to change. While harvest schedule could hypothetically be adjusted seasonally, the current model is resolved at a yearly timescale and does not allow for seasonal changes in harvest schedule. Thus, these parameters are neither

variable nor uncertain and therefore are not necessary to include in the MCA. Furthermore, their inclusion would obscure the range of outcomes due to parameters that are truly variable or uncertain. This is consistent with guidance found in the literature [51].

3. Techno-economic Analysis Results

After the probabilistic input parameters and their distributions were chosen, the MCA process was carried out using the @RISK software. Parameters with 5% or greater impact on either the TEA or LCA results were replaced with probabilistic distributions based on experimental or literature data, and the model was simulated for 5,000 iterations. The TEA results for both product configurations are shown in Figure 6 and Figure 7. The TEA MCA results, presented as histograms, are compared to the non-stochastic scenario analysis estimates in Figure 6. Then, the per-module costs are shown in Figure 7, for the three scenario analysis estimates as well as the 5th and 95th percentile results from the MCA.

The difference in shape between the two distributions in Figure 6 is due to the large range in methyl laurate market value. As discussed in section 1 and highlighted in Figure 4, the methyl laurate market value greatly affects the fuel selling price in the fuels and co-products case. This parameter widens the output range such that some scenarios have selling prices less than the fuels case, but most are still greater than the fuels case. The per-module breakdowns in Figure 7 show similar results as Figure 4 – the cultivation and methyl laurate harvest modules dominate the economics across all scenarios.

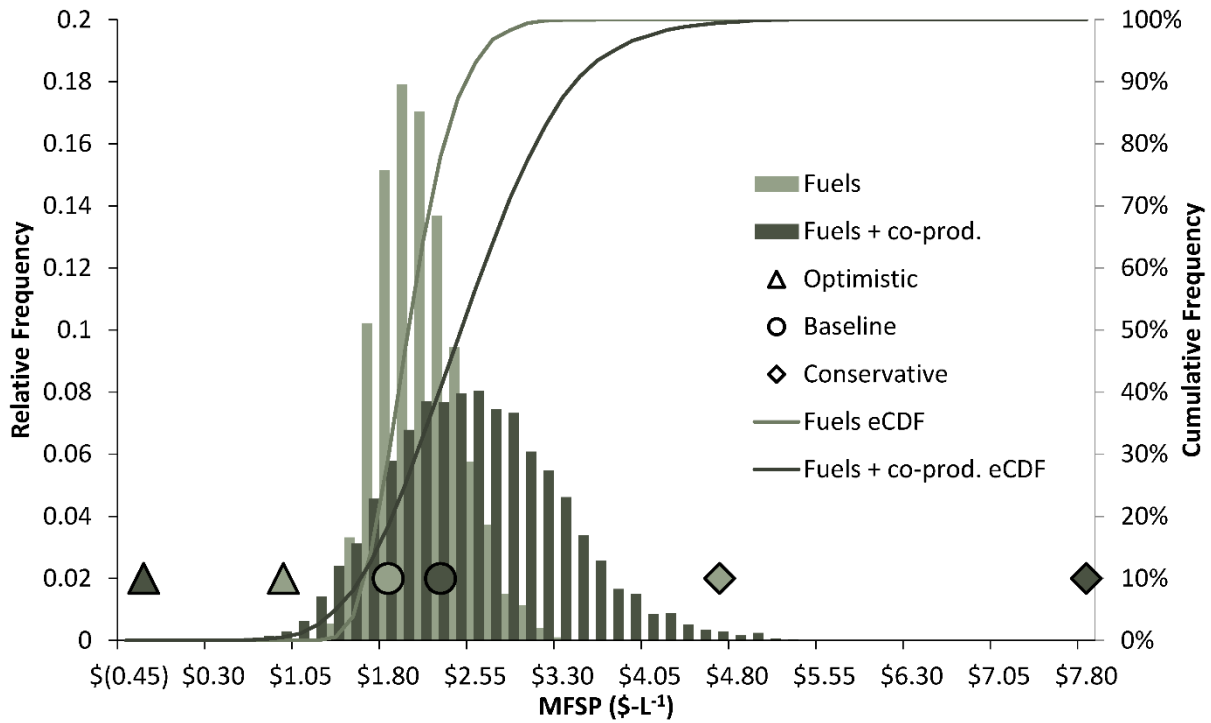


Figure 6: MCA results for MFSP presented as a dual histogram, compared to the static estimates presented with points. The lighter histogram and shapes correspond to the case of methyl laurate being sold as biodiesel, while the darker histogram and shapes correspond to the case of methyl laurate being sold as an oleochemical co-product. The shapes denote the non-stochastic (static) conservative, baseline and optimistic scenario estimates. The lines denote the empirical cumulative distribution function (eCDF), or cumulative frequency, which is equivalent to the empirical non-exceedance probability at the corresponding MFSP on the x-axis.

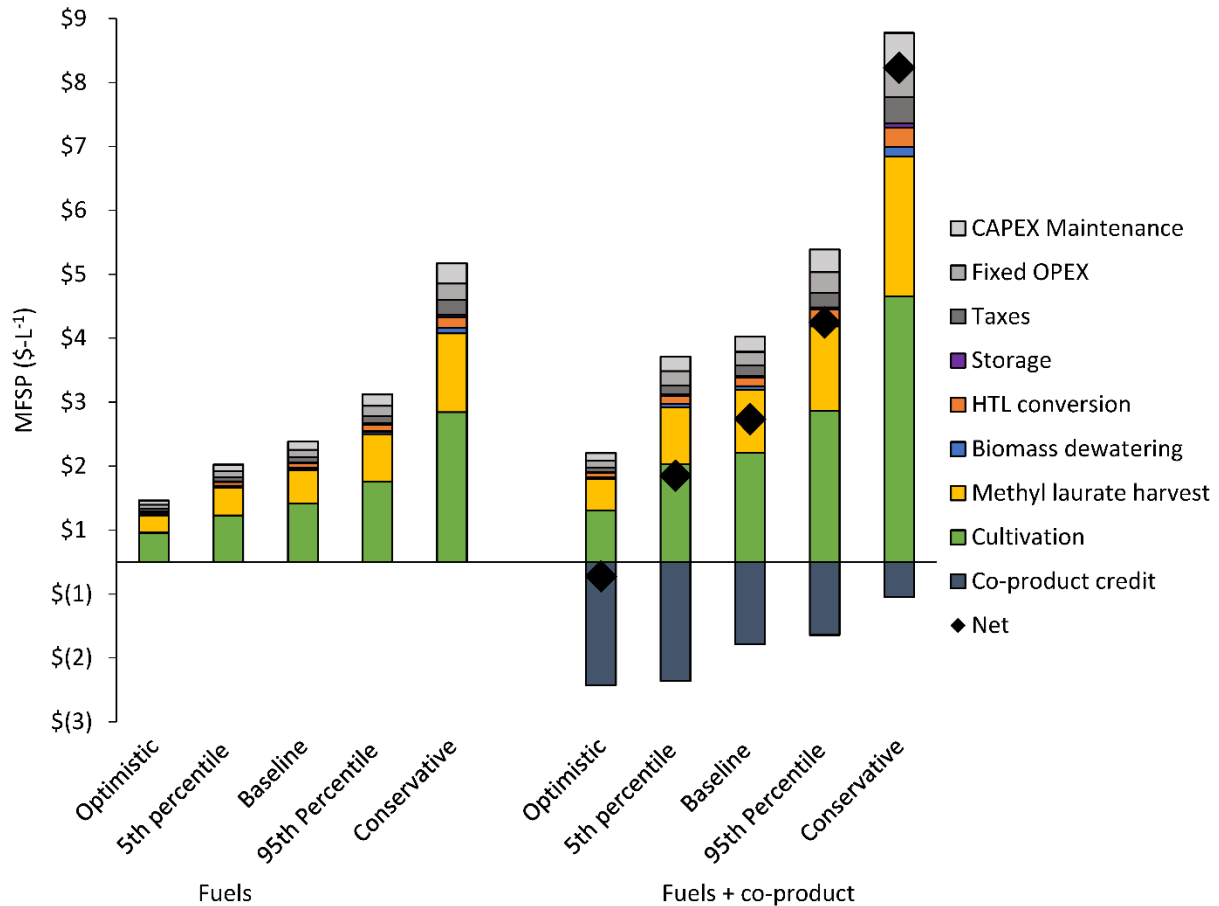


Figure 7: Facility breakdowns for CAPEX and OPEX for the baseline, optimistic, conservative, 5th and 95th percentile scenarios. For scenarios with co-product credits, the net result is shown with a black diamond.

3.1 Fuels case

Comparison between the MCA and non-stochastic (static scenario) results is the first means of analysis presented in this work. The MCA results for the fuels case (Figure 6) show a large range in MFSP, between $\$1.21\text{-L}^{-1}$ ($\$4.55\text{-gge}^{-1}$) and $\$3.48\text{-L}^{-1}$ ($\$13.63\text{-gge}^{-1}$), with an average MCA result of $\$2.01\text{-L}^{-1}$ ($\$7.60\text{-gge}^{-1}$). The static scenario results suggest even a larger range, with respective optimistic and conservative results of $\$0.96\text{-L}^{-1}$ ($\$3.64\text{-gge}^{-1}$) and $\$4.67\text{-L}^{-1}$ ($\$17.67\text{-gge}^{-1}$). These differences demonstrate the extreme compounding effect that scenario analysis has on the estimation of system outcomes. The 5th percentile in the fuels case varies

from the static baseline result by 19%, or 1.1 standard deviations. By contrast, the optimistic estimation varies from the static baseline by 49%, or 2.8 standard deviations. Even the minimum MCA result is just 2.0 standard deviations from the static baseline result (a 36% decrease). The effect is even more drastic in the conservative scenario, where the conservative estimate is 8.3 standard deviations from the static baseline result (a 150% increase), while the 95th percentile varies by 2.2 standard deviations (a 40% increase). Further, the conservative estimate is 1.3 times greater than the MCA maximum result. The large separation between the conservative and optimistic static scenario estimations and the tails of the MCA results are entirely due to the compounding effect of static scenario analysis. The optimistic and conservative scenarios are non-stochastic, and all input parameters are set to their respective best and worst-case values. This scenario analysis is standard practice in the literature and results in both under- and over-estimation of outcomes. The MCA reveals that it is extremely unlikely that all the best or worst values are randomly selected at the same time; this combination is never simulated by MCA, even in 10,000 iterations (refer to Figure A2 and Tables A5 and A6 for a comparison between the 5,000 and 10,000 iterations results).

In addition to avoiding the compounding effect of scenario analysis, MCA offers more refined insights for meeting performance targets. The economic benchmark for parity with conventional fuels is $\$0.80\text{-L}^{-1}$ (3-gge^{-1}). The MCA results on MFSP show that there is no iteration where the fuels scenario meets this benchmark. The approximate probability for meeting a more generous selling price of $\$1.32\text{-L}^{-1}$ ($\$5\text{-gge}^{-1}$) is 0.4%, which is estimated from the empirical non-exceedance probability, or the cumulative frequency. Investigating the 5th percentile result, considered to represent the minimum expected outcome, sheds light on the distance between current facility MFSP and economic targets. The 5th percentile scenario for the

fuels case is generated from several advantageous parameters: a high productivity of $13.9 \text{ g-m}^{-2}\text{-day}^{-1}$, a methyl laurate productivity ratio (the ratio of methyl laurate production to the cyanobacteria biomass) of 0.44 g-g^{-1} , and a bio-crude yield of 47%. The minimum scenario, with a MFSP of $\$1.21$ ($\$4.59\text{-gge}^{-1}$), has a biomass productivity of $15.0 \text{ g-m}^{-2}\text{-day}^{-1}$, methyl laurate production ratio of 0.45 g-g^{-1} , 53% bio-crude yield, and 359 operation days, all at the most advantageous end of their respective input distributions. Even with high productivities and operation days, the probability of meeting either economic target is very low – improvements to the parameters, shifting their respective input distributions to more advantageous ranges, is needed if economic parity is to be achieved.

The minimum and 5th percentile scenarios demonstrate a well-established aspect of microalgae biofuels research – that pond productivity is one of the most impactful parameters on facility economics [14]. Keeping all other parameters at baseline, increasing pond productivity to $25 \text{ g-m}^{-2}\text{-day}^{-1}$ brings the static baseline MFSP for the fuels case to $\$1.17\text{-L}^{-1}$ ($\$4.42\text{-gge}^{-1}$), and the estimated probability of meeting $\$0.80\text{-L}^{-1}$ increases from 0% to 0.02%. Adding to that a fixed methyl laurate production ratio of 0.5 g-g^{-1} , the static baseline MFSP for the fuels case decreases by 47% to $\$1.01\text{-L}^{-1}$ ($\$3.84\text{-gge}^{-1}$), and the same probability increases to 0.2%. An even larger increase to $35 \text{ g-m}^{-2}\text{-day}^{-1}$ (with the average methyl laurate production ratio of 0.375 g-g^{-1}), yields a static baseline MFSP of $\$0.92\text{-L}^{-1}$ ($\$3.50\text{-gge}^{-1}$), a 51% decrease from the original baseline result. It is noted that this scenario produces similar results to that of a $25 \text{ g-m}^{-2}\text{-day}^{-1}$ pond productivity and a methyl laurate production ratio of 0.5 g-g^{-1} . This highlights a unique quality of cyanobacteria – economic parity can be targeted through more manageable improvements of both carbon pathways, instead of very large improvements to the biomass productivity alone.

Another important economic parameter highlighted in the 5th percentile and minimum iterations is bio-crude yield, which directly influences the volume of fuel produced. Thus, increases in yield lead to decreases in MFSP. The most cost-competitive outcomes (5th percentile or better) have bio-crude yields greater than 35%, and average yields of 48%. Bio-crude yield varies widely [46] and little research has been done on HTL with cyanobacterial biomass. Better defining this parameter would greatly benefit future sustainability studies.

3.2 *Fuels and co-product case*

The effect of static scenario analysis compared to the stochastic approach of MCA is demonstrated in similar fashion in this case as was described in the fuels case. The 5th percentile result ($\$1.35\text{-L}^{-1}$) is 1.2 standard deviations or a 39% decrease from the static baseline result. In comparison, the optimistic result ($-\$0.22\text{-L}^{-1}$) is 3.4 standard deviations away, a 110% decrease from the static baseline result. The minimum MCA result of $\$0.27\text{-L}^{-1}$ is an 87% decrease from the static baseline. Likewise, the conservative estimate ($\$7.73\text{-L}^{-1}$) is 7.5 standard deviations from the static baseline, a 246% increase, compared to the 95th percentile outcome ($\$3.74\text{-L}^{-1}$) at 2.1 standard deviations, which is a 67% increase. The conservative estimate is two times larger than the 95th percentile result, and 1.4 times larger than the maximum MCA result. The fuels and co-product case has a larger range than the fuels case due to the large variation of the methyl laurate market value, which is not a factor in the fuels case. It is notable that the static baseline result, generated from the average input values, and the average output value of MCA are slightly different. This is due to the same phenomenon, with static combinations of inputs not precisely describing the stochastic outputs. However, these values are similar enough that the static baseline scenario is a reasonable representation of a central expected outcome for the purposes of investigating module-specific contributions.

The fuels and co-products case has better prospects for achieving economic parity than the fuels case due to the production of a high-value co-product. According to the MCA results, there is a 0.3% estimated probability of meeting the $\$0.80\text{-L}^{-1}$ ($\$3.00\text{-gge}^{-1}$) benchmark for the co-product case. This probability increases to 4.5% for a target of $\$1.32\text{-L}^{-1}$ ($\$5\text{-gge}^{-1}$). In a similar analysis to the fuels case, the 5th percentile and minimum MCA results yield insights to targets for the various input parameters towards meeting economic goals. The 5th percentile outcome is generated from a productivity of $14.0\text{ g-m}^{-2}\text{-day}^{-1}$, a methyl laurate production ratio of 0.41 g-g^{-1} , bio-crude yield of 36%, 333 operation days, and a methyl laurate market value of $\$2.10\text{-kg}^{-1}$. The minimum outcome has similarly high productivities of $14.9\text{ g-m}^{-2}\text{-day}^{-1}$ and 0.48 g-g^{-1} , bio-crude yield of 45%, 340 operation days, and a methyl laurate value of $\$2.51\text{-kg}^{-1}$. Outcomes with fuel selling prices of $\$0.80\text{-L}^{-1}$ or less have average pond productivities of $14.2\text{ g-m}^{-2}\text{-day}^{-1}$, methyl laurate production ratios of 0.47 g-g^{-1} , 45% bio-crude yield, 332 operation days, and methyl laurate market values of $\$2.53\text{-kg}^{-1}$. Importantly, fuel selling price outcomes less than or equal to $\$0.80\text{-L}^{-1}$ that have a low value for one parameter have advantageous values for the other parameters.

As noted in section 1 and in the results described above, pond productivities are the most important parameter to leverage for targeting economic parity. An increase in average productivity to $25\text{ g-m}^{-2}\text{-day}^{-1}$ yields a static baseline MFSP of $\$0.89\text{-L}^{-1}$ ($\$3.39\text{-gge}^{-1}$) and the probability of meeting the $\$0.80\text{-L}^{-1}$ benchmark increases to 32%. An additional increase in the methyl laurate production ratio to 0.5 g-g^{-1} decreases the baseline MFSP by 79% to $\$0.47\text{-L}^{-1}$ ($\$1.79\text{-gge}^{-1}$), and the probability increases to 65%. While the fuels case is highly unlikely to meet the economic benchmark, even with very large increases to the productivity of both products, the fuels and co-products case becomes much more advantageous with the same

increases. Setting the baseline productivity to $35 \text{ g}\cdot\text{m}^{-2}\cdot\text{day}^{-1}$ (and maintaining the original baseline methyl laurate production ratio) yields a static baseline MFSP of $\$0.44\cdot\text{L}^{-1}$ ($\$1.67\cdot\text{g}\cdot\text{g}^{-1}$), an 80% decrease from the original baseline result. Like the fuels case, this scenario is very similar to the one described before ($25 \text{ g}\cdot\text{m}^{-2}\cdot\text{day}^{-1}$ pond productivity and $0.5 \text{ g}\cdot\text{g}^{-1}$ methyl laurate production ratio), demonstrating the unique benefit of cyanobacteria with secreted products. This productivity analysis is consistent with Somers and Quinn [42] and Cruce et al. [14], who find that such increases yield much more advantageous MFSPs and are crucial for achieving economic parity with fossil fuels.

Bio-crude yield also affects facility economics, but to a lesser extent than the fuels case. The 5th percentile or better outcomes are generated from average bio-crude yields of 45%, although yields across the full input range are present. Regardless, as demonstrated by the sensitivity analysis results in section 2, bio-crude yield is an impactful parameter that should be more precisely defined by future studies.

The principal conclusions highlighted by these results address both modeling methods and improvements towards sustainability targets. First, while static scenario analysis can be useful for a preliminary approach to addressing system variability, simulating a random combination of scenarios via MCA is a far more realistic portrait of system outcomes. Static scenarios should at most be considered extreme bounds of the expected outcomes, and should not be cited as results one should expect in application of the modeled technology. Second, increases in productivity are absolutely imperative for achieving economic feasibility. Encouragingly, cyanobacteria pose an opportunity for bio-engineering more moderate improvements to both biomass productivity and secreted volumes that achieve similar targets as microalgae with very ambitious improvements to biomass productivity alone. Other important

input parameters include bio-crude yield and methyl laurate market value – both of which have meaningful effects on the system economics. More refined data are needed in order to better define their ranges.

4. Life Cycle Assessment Results

The MCA on GWP was run with the same probabilistic inputs for process parameters as the TEA, which are outlined in Tables A2, A3 and A4 of the supplementary information. The economic and environmental results are produced with the same MCA iterations, so each economic result in Figure 6 has a complimentary environmental result in Figure 8. The histogram of MCA results is shown in Figure 8, which also includes points for the static conservative, baseline and optimistic scenario results for each case. The per-module facility results for the 5th and 95th percentile MCA results and the three static scenario analyses are shown in Figure 9.

The shapes of the distributions for the two cases in Figure 8 are very similar as the methyl laurate market value has a much smaller impact on the environmental results than the economic. Thus, the two systems have nearly the same shape, and the fuels and co-products case outcomes are shifted approximately 20 g CO₂-eq-MJ⁻¹ higher due to the economic allocation of impacts and the reduced volume of fuels being produced. The per-module results for the illustrated scenarios reflect that of the baseline results shown in Figure 3 – methyl laurate harvest and HTL conversion account for a large part of the burden after the combustion of the fuel products. These are partially offset by large carbon uptake credits from the CO₂ absorbed by the pond.

The difference in the MCA tails and the optimistic and conservative scenario estimates are slightly less pronounced in the LCA compared to the TEA. Put simply, the LCA is less

sensitive than the TEA, and therefore undergoes smaller changes with the same variation on inputs. This is because LCA methodology only addresses operational consumables, analogous to the OPEX in the TEA. However, there is no equivalent to CAPEX in the LCA. While embedded emissions of the various equipment throughout the facility can be considered, they were not included in the scope of this study as they are expected to be small when amortized over the 30-year life of the system. Because of this, the LCA results are inherently less sensitive, and therefore have less extreme distances between the tails of MCA and the static scenario estimates, especially on the optimistic side of the distribution.

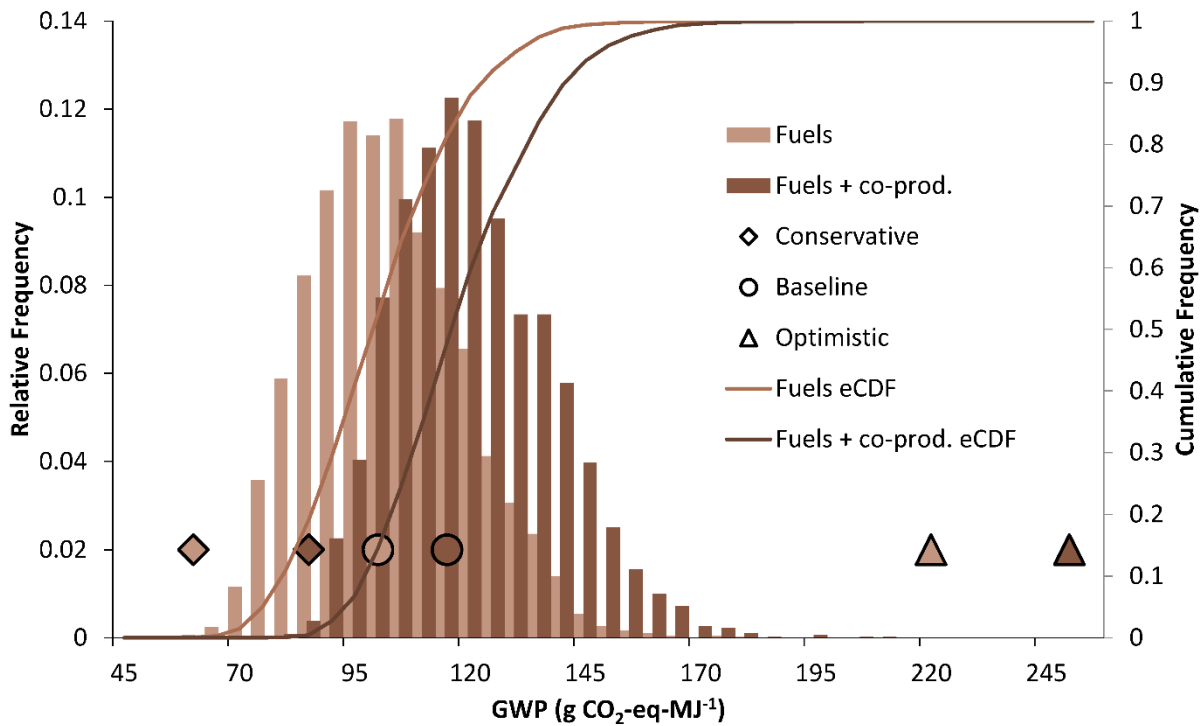


Figure 8: MCA results for GWP in the histogram, compared to the static estimates, illustrated with shapes. The lighter histogram and shapes correspond to the fuels case, and the darker histogram and shapes correspond to the fuels and co-products case. The optimistic, baseline, and conservative static scenario estimates are represented with triangles, circles and diamonds, respectively. The lines denote the empirical cumulative distribution function (eCDF), or cumulative frequency, which is equivalent to the empirical non-exceedance probability at the corresponding MFSP on the x-axis.

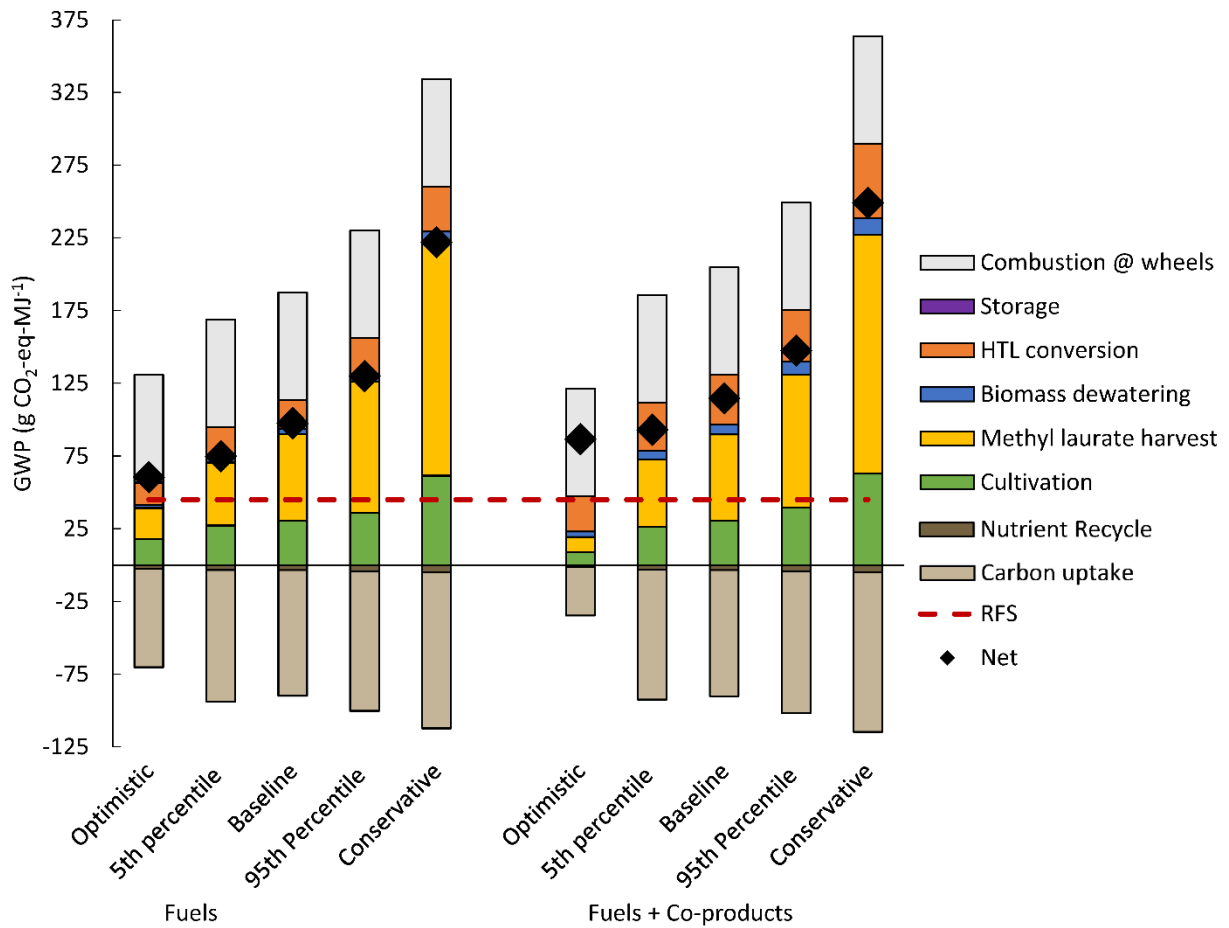


Figure 9: Facility breakdown of GWP, with the net results represented with the black diamonds. The dashed red line represents the renewable fuel standard (RFS), which is half the GWP of petroleum at 45 g-CO₂-eq-MJ⁻¹.

4.1 Fuels case

The static optimistic result (61 g CO₂-eq-MJ⁻¹) is 2.2 standard deviations from the static baseline result of 98 g CO₂-eq-MJ⁻¹, or a 38% decrease. In comparison, the 5th percentile result (75 g CO₂-eq-MJ⁻¹) is a 23% decrease from the baseline, and the minimum result (59 g CO₂-eq-MJ⁻¹) is a 39% decrease. Likewise, the static conservative result of 222 g CO₂-eq-MJ⁻¹ is 7.5 standard deviations from the static baseline result, a 127% increase. The 95th percentile result (130 g CO₂-eq-MJ⁻¹) is only a 33% increase from the static baseline result, while the maximum

MCA result ($175 \text{ g CO}_2\text{-eq-MJ}^{-1}$) is a 79% increase. These relative differences are similar to those of the TEA, especially on the conservative side of the histogram.

It is important to note that the 5th and 95th percentile results for the LCA do not occur under the same set of input values as the TEA. The 5th percentile MFSP for the fuels case corresponds with the approximate 51st percentile LCA result and the 95th MFSP result corresponds with the approximate 98th percentile LCA result. Reversed, the inputs generating the 5th percentile GWP result yield approximately the 10th percentile MFSP result and those associated with the 95th percentile GWP generate the approximate 99th percentile MFSP result. In general, what is expensive is also energetically intensive and is linked with larger environmental burdens. However, certain parameters such as methyl laurate market value or electricity cost can reduce the MFSP while the GWP remains high.

The renewable fuel standard is a GWP of $45 \text{ g CO}_2\text{-eq-MJ}^{-1}$, which is half that of petroleum [57]. The results show there is no outcome that currently meets the renewable fuel standard for this case. The lowest 5% of results, which have GWPs of 59 to $75 \text{ g CO}_2\text{-eq-MJ}^{-1}$ for the fuels case, have average productivities of $14 \text{ g-m}^{-2}\text{day}^{-1}$ and methyl laurate production ratios of 0.45 g-g^{-1} , both at the upper end of their input ranges. As demonstrated in the economic results and other work, high productivities have a decreasing effect on the environmental impacts [14]. Increasing the baseline productivity to $25 \text{ g-m}^{-2}\text{day}^{-1}$ brings the environmental impact to $62 \text{ g CO}_2\text{-eq-MJ}^{-1}$ (a 36% decrease), and an additional increase to the baseline methyl laurate production ratio to 0.5 g-g^{-1} , brings the fuels footprint to $55 \text{ g CO}_2\text{-eq-MJ}^{-1}$ (a 44% decrease). An increase in productivity to $35 \text{ g-m}^{-2}\text{-day}^{-1}$, keeping the methyl laurate production ratio at baseline, results in a GWP of $50 \text{ g CO}_2\text{-eq-MJ}^{-1}$, which is just over half the original baseline GWP. The same effect is present as in the TEA – large increases to productivity alone have

similar resulting gains as more moderate increases to that of both the biomass and secreted product. While these improvements bring the footprint below that of petroleum's (90 g CO₂-eq-MJ⁻¹), they are not sufficient for meeting the RFS.

Another impactful parameter to the facility environmental impact is carbon utilization, which has a slightly stronger effect on the environmental results than the economic ones. The lowest 5% of the GWP for both cases have average utilization rates of 25%, slightly higher than the average utilization efficiency input. CO₂ is the primary feedstock to the growth ponds, and current utilization rates are between 20% and 40%. Notably, energy requirements, and therefore environmental impact, do not increase linearly with off-gassing. As utilization rate decreases, especially below 10%, the energy requirement to deliver adequate carbon increases exponentially, impacting both the environmental and economic impacts. Utilization efficiency is not well-defined in the literature, with assumptions ranging from 0% [32] to 90% [15], [42]. According to this model, rates of at least 20% should be targeted for improved fuel impacts.

Bio-crude yield impacts the environmental and economic results differently – while increases in yield correspond with decreases in MFSP, they have the opposite effect on GWP. An increase in bio-crude yield increases the fuel yield and the amount of carbon released from combustion, making the GWP of the facility larger. Further, as yield decreases, the aqueous material returned to the ponds increases, increasing the carbon credit for recycled nutrients. For the lowest 5% GWP, average yields for both cases (37% and 42%) are lower than those of the lowest 5% of MFSP results, where bio-crude yield rates were generally at the higher end of the simulated range. This is also why the distances between the static optimistic and the minimum MCA results are much smaller in both cases – the optimistic and conservative bio-crude yields are opposite for the TEA and LCA. Setting the optimistic bio-crude yield input to the

conservative value (30%) decreases the optimistic scenario result to 49 g CO₂-eq-MJ⁻¹, a 19% decrease from the original optimistic result. This change also widens the percent change from the static baseline result to 50%. Practically, this result is uncomplicated – the more fuels are produced and combusted, the higher the GWP will be. However, this is a compelling result that highlights the trade-off between economic feasibility and environmental burden. Incorporating policies such as financial credits for carbon uptake can likely help alleviate this conflict between economic and environmental impacts, although investigating those implications were outside the scope of this work.

4.2 *Fuels and co-product case*

In a similar analysis to the fuels case, the static conservative estimate (249 g CO₂-eq-MJ⁻¹) is 7.9 standard deviations or a 117% increase from the static baseline result. This is compared to that of the 95th percentile result (148 g CO₂-eq-MJ⁻¹) which is 1.9 standard deviations away, or a 29% increase from the static baseline result. The distance between the static optimistic result (87 g CO₂-eq-MJ⁻¹) and the static baseline result is just 1.6 standard deviations, equivalent to a 24% decrease. The 5th percentile result (93 g CO₂-eq-MJ⁻¹) is similar, 1.3 standard deviations from the baseline and a 19% decrease. The distance between the optimistic and 5th percentile results and the baseline scenario is much smaller than that of the conservative and 95th percentile results – this is due to the economic allocation methodology, discussed later in this section.

Similar to the fuels results, none of the simulated scenarios meet the renewable fuel standard of 45 g CO₂-eq-MJ⁻¹. The lowest 5% of results, with GWPs of 77 to 93 g CO₂-eq-MJ⁻¹, have the same average productivities as the fuels case: approximately 14 g-m⁻²day⁻¹ pond productivity and methyl laurate production ratios of 0.45 g-g⁻¹. Bringing the baseline productivity to 25 g-m⁻²day⁻¹ decreases the environmental impact by 32% to 78 g CO₂-eq-MJ⁻¹.

Adding to that an approximate 50% methyl laurate production ratio increase to 0.5 g-g^{-1} brings the fuels footprint to $74 \text{ g CO}_2\text{-eq-MJ}^{-1}$ for the fuels and co-products case. A large (61%) increase in biomass productivity to $35 \text{ g-m}^{-2}\text{-day}^{-1}$ brings the fuels footprint to $66 \text{ g CO}_2\text{-eq-MJ}^{-1}$, a 42% decrease from the original baseline. This is a larger difference from the $25 \text{ g-m}^{-2}\text{-day}^{-1}$ and 0.5 g-g^{-1} combination because increasing the biomass productivity creates a larger relative fuel yield when the methyl laurate is being treated as a co-product. Therefore, there are larger gains between these two scenarios than when the methyl laurate is being treated as a fuel product.

The methyl laurate market value is the only economic parameter with bearing in the GWP calculation for the fuels and co-product case, due to the economic allocation method for the assignment of emissions to the two products. As described in section 3 of the methods, the impacts of the cultivation and harvest modules are assigned to the two products according to their economic value. This allocation method is generally most advantageous for the fuels' footprint when the methyl laurate has a higher economic value. In the lowest 5% of the GWP results for the fuels and co-product case, the average methyl laurate market value is $\$1.52\text{-kg}^{-1}$, while the value of the fuel products is $\$1\text{-kg}^{-1}$ ($\$3\text{-gge}^{-1}$). Increasing the methyl laurate market value returns small gains in GWP: a value of $\$3\text{-kg}^{-1}$ negligibly decreases the fuels footprint to $114 \text{ g CO}_2\text{-eq-MJ}^{-1}$, while the methyl laurate footprint increases to $4 \text{ g CO}_2\text{-eq-MJ}^{-1}$ to compensate. The methyl laurate market value has limited effect on the GWP of the fuels, since the portion of the facility being allocated is almost completely off-set by the carbon uptake. After accounting for the carbon uptake credit, the downstream processing modules make up the largest portion of the emissions and are totally allocated to the fuels. Thus, the fuels take on a majority of the facility emissions, regardless of the methyl laurate market value. This is confirmed by the

fact that the methyl laurate market value has just a 1% impact on GWP, according to the sensitivity analysis.

Despite the small effect of the methyl laurate economic value on the GWP outcomes, it is important to discuss the implications of emissions allocation in this work. Emissions allocation is a complex aspect of LCA in biorefining systems that produce a concurrent non-fuel co-product – it is impossible to know the true impact of the product unless its entire life cycle is known. For a facility producing an oleochemical that can be used in any number of processes or products, prescribing its end uses, disposal and lifetime is not possible. Allocation methods attempt to remedy this issue by assigning proportions of facility impacts to the various products according to either their mass, energy content, or economic value. Economic allocation has been chosen to account for the products' respective impacts, which decreases the fuels impact as the economic value of the methyl laurate increases. As the co-product's value increases, it takes on a larger portion of the facility's burdens, effectively decreasing the fuels impact. This relationship reverses when the facility impacts are net negative (before combustion of the fuel products), such as in the case of large uptake credits for high carbon utilization rates and biomass productivities. In that case, as the co-product value increases and the portion of impacts allocated to the fuels decreases, the fuels impact increases. Reversed, for a low co-product value that allocates more of the burden to the fuels, the fuels impact decreases since the "burden" is in fact negative. While this is mathematically consistent, the method breaks down conceptually. Effectively, this relationship is suggesting that the best practice in the case of a net-negative facility emissions is to sell the co-product for as little as possible, which results in the lowest possible impact for the fuels. This is backward from what high-value co-products usually achieve. This result is more an artifact of the allocation method than it is a reflection of the realistic impacts of either product.

Further, LCA allocation is an imperfect, hypothetical way of assigning impacts and is not well-suited to facility scenarios with net-negative impacts. While allocation cannot often be avoided altogether, it has the potential to obscure the true amount of emissions. Therefore, transparent reporting of the original facility emissions and the applied allocation methods is of utmost importance.

To summarize the LCA results, while the fuels case gets closer to the RFS than the fuels and co-products case, neither product configuration meets it, illustrating that meeting environmental benchmarks poses an even larger challenge to cyanobacterial biofuels than achieving economic parity. Furthermore, the LCA results are less sensitive than the TEA, so reducing facility emissions towards the RFS will require more systemic adjustments rather than point-source improvements. For example, targeting a facility run partially or completely on clean energy would be much more effective than specific parameter improvements. Even so, productivity increases to both the biomass and the secreted methyl laurate are worth pursuing considering their shared significant effects on the environmental and economic impacts of the facility.

5. Discussion of MCA methodology

While software such as @RISK make executing MCA relatively straightforward, it cannot guarantee that the input data are sufficient for an adequate reflection of the system. It is the user's responsibility to ensure that the input distributions being applied are adequately reflecting the input parameters, which is ultimately dependent on data availability. The distribution fitting tool in @RISK compares multiple fitting criteria and allows the user to select fitted distributions to a given data set based on method. However, the tool is only as accurate as the data set being used as a basis. Without adequate data, the chosen probability distribution will

almost certainly be inaccurate. Data should both be relevant and in high enough supply – sample sizes must be large enough to extract meaningful statistics.

While input distributions generated from large data sets are ideal, that is simply not an option for many aspects of the first of a kind technology inherent in the process modeling of algae biorefining. It is in these cases that less specific input distributions be employed, such as triangular and uniform distributions, which are better suited to parameters with limited to no data. The present study uses uniform distributions for process inputs that do not have sufficient experimental data, which assume all values in the range have equal probability. Where possible, efforts should be made to survey available data and generate meaningful input distributions. However, assigning uniform distributions to every parameter still avoids the compounding issue of scenario analysis. As this study has demonstrated, the conservative scenario for TEA can be up to twice as large as the 95th percentile result, with similar trends on the optimistic side. The same trend is observed for the LCA results, but to a lesser extent. Avoiding this compounding effect will surely lead to more realistic and informative results going forward.

The MCA in this work was heavily based on the results of the sensitivity analysis. As described in section 4.1, inputs highlighted by the sensitivity as high-impact were given probabilistic input distributions. Importantly, these parameters were identified via a first-order analysis that captured the impacts of individual parameters but not the interactions between parameters. Capturing the latter form of sensitivity requires a global sensitivity analysis, or an “all-[factors]-at-a-time” approach, as described by Pianosi, et al. [30]. This type of sensitivity analysis is a more complex approach that can highlight additional parameters not captured by the local sensitivity analysis. Integrating second-order sensitivity analysis was outside the scope of this work, and it is reasonable to assume that the majority of impactful parameters were captured

in the first-order sensitivity. However, second-order sensitivity should be included in future work to ensure that all influential parameters, both local and global, are being given probabilistic input distributions in the MCA.

CONCLUSIONS

The present study evaluates the environmental impact and economic feasibility of a cyanobacteria-to-products facility that generates fuels and a methyl laurate oleochemical. The economic and environmental outcomes are first limited by productivity. Increases in both biomass and methyl laurate productivities would greatly benefit the system toward meeting the \$0.80-L⁻¹ benchmark and reducing the GWP of the fuels. The environmental burden is also disadvantaged by the high off-gassing of delivered CO₂, increasing an already energetically intensive process. Finally, the bio-crude yield oppositely affects the economic and environmental outcomes, with increases correlated with decreases in MFSP but increases in GWP. Higher productivity rates could potentially offset incremental increases in bio-crude yield in favor of more feasible MFSP and GWP.

There are two methodological findings of this study. First, that MCA is a useful alternative for addressing variability and uncertainty that avoids the maximization and minimization of static scenario analysis. It is reasonably straightforward to implement, and while using many or all uniform distributions sacrifices some of the probabilistic information, it is still a more realistic portrait of the facility outcomes than a non-stochastic analysis. Additionally, more specific probability distributions should be informed with adequate data. The second methodological finding is that LCA allocation methods are not well-suited to net-negative facility emissions. They should be avoided when possible and applied transparently when necessary.

REFERENCES

- [1] “Greenhouse Gas Emissions: Sources of Greenhouse Gas Emissions,” *United States Environmental Protection Agency*, 2020. [Online]. Available: <https://www.epa.gov/ghgemissions/sources-greenhouse-gas-emissions>. [Accessed: 28-Jan-2021].
- [2] P. Collet, A. Hélias, L. Lardon, J. P. Steyer, and O. Bernard, “Recommendations for Life Cycle Assessment of algal fuels,” *Appl. Energy*, vol. 154, pp. 1089–1102, 2015.
- [3] A. Singh and S. I. Olsen, “A critical review of biochemical conversion, sustainability and life cycle assessment of algal biofuels,” *Appl. Energy*, vol. 88, no. 10, pp. 3548–3555, 2011.
- [4] E. Frank, A. Elgowainy, J. Han, and Z. Wang, “Life cycle comparison of hydrothermal liquefaction and lipid extraction pathways to renewable diesel from algae,” *Mitig. Adapt. Strateg. Glob. Chang.*, vol. 18, no. 1, pp. 137–158, 2013.
- [5] A. K. Pegallapati and E. D. Frank, “Energy use and greenhouse gas emissions from an algae fractionation process for producing renewable diesel,” *Algal Res.*, vol. 18, pp. 235–240, 2016.
- [6] C. H. Sun *et al.*, “Life-cycle assessment of biofuel production from microalgae via various bioenergy conversion systems,” *Energy*, vol. 171, pp. 1033–1045, 2019.
- [7] K. DeRose, C. DeMill, R. W. Davis, and J. C. Quinn, “Integrated techno economic and life cycle assessment of the conversion of high productivity, low lipid algae to renewable fuels,” *Algal Res.*, vol. 38, no. July 2018, p. 101412, 2019.
- [8] B. D. Beckstrom and J. C. Quinn, “Bioplastic production from microalgae with fuel co-

- prducts: a techno-economic and life-cycle assessment,” Fort Collins, CO, 2019.
- [9] I. M. P. Machado and S. Atsumi, “Cyanobacterial biofuel production,” *J. Biotechnol.*, vol. 162, no. 1, pp. 50–56, 2012.
- [10] V. O. Adesanya, E. Cadena, S. A. Scott, and A. G. Smith, “Life cycle assessment on microalgal biodiesel production using a hybrid cultivation system,” *Bioresour. Technol.*, vol. 163, pp. 343–355, 2014.
- [11] A. Parmar, N. K. Singh, A. Pandey, E. Gnansounou, and D. Madamwar, “Cyanobacteria and microalgae: A positive prospect for biofuels,” *Bioresour. Technol.*, vol. 102, no. 22, pp. 10163–10172, Nov. 2011.
- [12] P. Farrokh, M. Sheikhpour, A. Kasaeian, H. Asadi, and R. Bavandi, “Cyanobacteria as an eco-friendly resource for biofuel production: A critical review,” *Biotechnol. Prog.*, vol. 35, no. 5, pp. 1–16, 2019.
- [13] B. T. Nguyen, B. E. Rittmann, R. Krajmalnik-Brown, and P. Westerhoff, “Photoautotrophic Production of Biomass, Laurate, and Soluble Organics by *Synechocystis* sp. PCC 6803,” 2015.
- [14] J. Cruce *et al.*, “Driving toward sustainable algal fuels: A harmonization of techno-economic and life cycle assessments,” *Algal Res.*, vol. 54, p. 102169, 2021.
- [15] R. Davis, J. Markham, C. Kinchin, N. Grundl, E. Tan, and D. Humbird, “Process Design and Economics for the Production of Algal Biomass: Algal Biomass Production in Open Pond Systems and Processing Through Dewatering for Downstream Conversion,” *Natl. Renew. Energy Lab.*, no. February, p. 128, 2016.
- [16] M. R. Tredici, L. Rodolfi, N. Biondi, N. Bassi, and G. Sampietro, “Techno-economic analysis of microalgal biomass production in a 1-ha Green Wall Panel (GWP®) plant,”

- Algal Res.*, vol. 19, pp. 253–263, 2016.
- [17] F. Fasaei, J. H. Bitter, P. M. Slegers, and A. J. B. van Boxtel, “Techno-economic evaluation of microalgae harvesting and dewatering systems,” *Algal Res.*, vol. 31, no. February, pp. 347–362, 2018.
- [18] R. Schneider, M. de Moura Lima, M. Hoeltz, F. de Farias Neves, D. K. John, and A. de Azevedo, “Life cycle assessment of microalgae production in a raceway pond with alternative culture media,” *Algal Res.*, vol. 32, no. October 2017, pp. 280–292, 2018.
- [19] S. Jones, Y. Zhu, D. Anderson, R. T. Hallen, and D. C. Elliott, “Process Design and Economics for the Conversion of Algal Biomass to Hydrocarbons : Whole Algae Hydrothermal Liquefaction and Upgrading,” 2014.
- [20] R. Davis *et al.*, “Process Design and Economics for the Conversion of Algal Biomass to Biofuels: Algal Biomass Fractionation to Lipid- and Carbohydrate-Derived Fuel Products,” 2014.
- [21] Y. Zhu, S. B. Jones, A. J. Schmidt, K. O. Albrecht, S. J. Edmundson, and D. B. Anderson, “Techno-economic analysis of alternative aqueous phase treatment methods for microalgae hydrothermal liquefaction and biocrude upgrading system,” *Algal Res.*, vol. 39, no. September 2018, p. 101467, 2019.
- [22] E. P. Bennion, D. M. Ginosar, J. Moses, F. Agblevor, and J. C. Quinn, “Lifecycle assessment of microalgae to biofuel: Comparison of thermochemical processing pathways,” *Appl. Energy*, vol. 154, pp. 1062–1071, Sep. 2015.
- [23] T. J. Johnson *et al.*, “Producing next-generation biofuels from filamentous cyanobacteria: An economic feasibility analysis,” *Algal Res.*, vol. 20, pp. 218–228, 2016.
- [24] J. N. Markham *et al.*, “Techno-economic analysis of a conceptual biofuel production

- process from bioethylene produced by photosynthetic recombinant cyanobacteria,” *Green Chem.*, vol. 18, no. 23, pp. 6266–6281, 2016.
- [25] C. Quiroz-Arita, J. J. Sheehan, and T. H. Bradley, “Life cycle net energy and greenhouse gas emissions of photosynthetic cyanobacterial biorefineries: Challenges for industrial production of biofuels,” *Algal Res.*, vol. 26, pp. 445–452, Sep. 2017.
- [26] A. Nilsson, K. Shabestary, M. Brandão, and E. P. Hudson, “Environmental impacts and limitations of third-generation biobutanol: Life cycle assessment of n-butanol produced by genetically engineered cyanobacteria,” *J. Ind. Ecol.*, vol. 24, no. 1, pp. 205–216, 2020.
- [27] S. Smetana, M. Sandmann, S. Rohn, D. Pleissner, and V. Heinz, “Autotrophic and heterotrophic microalgae and cyanobacteria cultivation for food and feed: life cycle assessment,” *Bioresour. Technol.*, vol. 245, no. August, pp. 162–170, 2017.
- [28] A. T. Ubando, J. L. Cuello, M. M. El-Halwagi, A. B. Culaba, M. A. B. Promentilla, and R. R. Tan, “Application of stochastic analytic hierarchy process for evaluating algal cultivation systems for sustainable biofuel production,” *Clean Technol. Environ. Policy*, vol. 18, no. 5, pp. 1281–1294, 2016.
- [29] J. Hoffman, R. C. Pate, T. Drennen, and J. C. Quinn, “Techno-economic assessment of open microalgae production systems,” *Algal Res.*, vol. 23, pp. 51–57, 2017.
- [30] F. Pianosi *et al.*, “Sensitivity analysis of environmental models: A systematic review with practical workflow,” *Environ. Model. Softw.*, vol. 79, pp. 214–232, 2016.
- [31] L. Y. Batan, G. D. Graff, and T. H. Bradley, “Techno-economic and Monte Carlo probabilistic analysis of microalgae biofuel production system,” *Bioresour. Technol.*, vol. 219, pp. 45–52, 2016.
- [32] P. Pérez-López, M. Montazeri, G. Feijoo, M. T. Moreira, and M. J. Eckelman,

- “Integrating uncertainties to the combined environmental and economic assessment of algal biorefineries: A Monte Carlo approach,” *Sci. Total Environ.*, vol. 626, pp. 762–775, 2018.
- [33] D. L. Sills *et al.*, “Quantitative uncertainty analysis of life cycle assessment for algal biofuel production,” *Environ. Sci. Technol.*, vol. 47, no. 2, pp. 687–694, 2013.
- [34] A. T. Ubando, J. L. Cuello, A. B. Culaba, M. A. B. Promentilla, and R. R. Tan, “Multi-criterion evaluation of cultivation systems for sustainable algal biofuel production using analytic hierarchy process and Monte Carlo simulation,” *Energy Procedia*, vol. 61, pp. 389–392, 2014.
- [35] M. O. P. Fortier, G. W. Roberts, S. M. Stagg-Williams, and B. S. M. Sturm, “Life cycle assessment of bio-jet fuel from hydrothermal liquefaction of microalgae,” *Appl. Energy*, vol. 122, no. July 2011, pp. 73–82, 2014.
- [36] J. W. Richardson, M. D. Johnson, and J. L. Outlaw, “Economic comparison of open pond raceways to photo bio-reactors for profitable production of algae for transportation fuels in the Southwest,” *Algal Res.*, vol. 1, no. 1, pp. 93–100, 2012.
- [37] J. W. Richardson, M. D. Johnson, R. Lacey, J. Oyler, and S. Capareda, “Harvesting and extraction technology contributions to algae biofuels economic viability,” *Algal Res.*, vol. 5, pp. 70–78, 2014.
- [38] J. Kern, A. M. Hise, G. W. Characklis, R. Gerlach, S. Viamajala, and R. D. Gardner, “Using life cycle assessment and techno-economic analysis in a real options framework to inform the design of algal biofuel production facilities,” *Bioresour. Technol.*, no. 225, pp. 418–428, 2016.
- [39] P. Cheali, J. A. Posada, and K. V. G. Gurkan Sin, “Economic risk analysis and critical

- comparison of optimal biorefinery concepts,” *Biofuels, Bioprod. Biorefining*, vol. 6, no. 3, pp. 246–256, 2012.
- [40] National Center for Biotechnology Information, “PubChem Compound Summary for CID 58150421,” *PubChem*, 2021. [Online]. Available: <https://pubchem.ncbi.nlm.nih.gov/compound/4-Nitroaniline#section=NIOSH-Toxicity-Data%0Ahttps://pubchem.ncbi.nlm.nih.gov/compound/58150421>.
- [41] R. Qiu, S. Gao, P. A. Lopez, and K. L. Ogden, “Effects of pH on cell growth, lipid production and CO₂ addition of microalgae *Chlorella sorokiniana*,” *Algal Res.*, vol. 28, no. Iv, pp. 192–199, 2017.
- [42] M. D. Somers and J. C. Quinn, “Sustainability of carbon delivery to an algal biorefinery: A techno-economic and life-cycle assessment,” *J. CO₂ Util.*, vol. 30, no. September 2018, pp. 193–204, 2019.
- [43] G. Last and M. Schmick, “Identification and Selection of Major Carbon Dioxide Stream Compositions,” no. June, p. 38, 2011.
- [44] G. Towler and R. Sinnott, *Chemical Engineering and Design: Principles, Practice and Economics of Plant and Process Design*, 2nd ed. Waltham, MA: Butterworth-Heinemann, Elsevier Ltd., 2013.
- [45] S. Edmundson *et al.*, “Phosphorus and nitrogen recycle following algal bio-crude production via continuous hydrothermal liquefaction,” *Algal Res.*, vol. 26, no. June, pp. 415–421, 2017.
- [46] P. H. Chen and J. C. Quinn, “Microalgae to biofuels through hydrothermal liquefaction: Open-source techno-economic analysis and life cycle assessment,” *Appl. Energy*, vol. 289, no. February, p. 116613, 2021.

- [47] T. Brown, *Engineering Economics and Economic Design for Process Engineers*. 2016.
- [48] G. Wernet, C. Bauer, B. Steubing, J. Reinhard, E. Moreno-Ruiz, and B. Weidama, “The ecoinvent database version 3 (part 1): overview and methodology,” *Int. Journal Life Cycle Assess.*, vol. 21, no. 9, pp. 1218–1230, 2016.
- [49] J. C. Bare, “Tool for the Reduction and Assessment of Chemical and Other Environmental Impacts (TRACI), Version 2.1 - User’s Manual.” US EPA, 2012.
- [50] Technical Committee ISO/TC 217, “Environmental management - Life cycle assessment - Requirements and guidelines.” p. 46, 2006.
- [51] US EPA, “Guiding Principles for Monte Carlo Analysis. EPA/630/R-97/001 March 1997. Risk Assessment Forum. Washington D.C. 20460. Available at: {<http://www2.epa.gov/sites/production/files/2014-11/documents/montecar.pdf>} (accessed May 2018),” no. March, p. 39, 1997.
- [52] “@Risk.” Palisade Company, LLC.
- [53] Palisade Company, “Palisade Knowledge Base: 4.14. Best Fit for Small Data Sets?,” 2015. [Online]. Available: <https://kb.palisade.com/index.php?pg=kb.page&id=998>. [Accessed: 03-Nov-2021].
- [54] Palisade Company, “Palisade Knowledge Base: 4.12. Interpreting AIC Statistics,” 2015. [Online]. Available: <https://kb.palisade.com/index.php?pg=kb.page&id=1070>. [Accessed: 03-Nov-2021].
- [55] S. H. Begg, M. B. Welsh, and R. B. Bratvold, “Uncertainty vs. Variability: What’s the Difference and Why is it Important?,” in *SPE Hydrocarbon Economics and Evaluation Symposium*, 2014.
- [56] M. A. J. Huijbregts, “Application of uncertainty and variability in LCA. Part I: A general

framework for the analysis of uncertainty and variability in life cycle assessment,” *Int. J. Life Cycle Assess.*, vol. 3, no. 5, pp. 273–280, 1998.

- [57] “Renewable Fuel Standard Program,” *US EPA*, 2017. [Online]. Available: <https://www.epa.gov/renewable-fuel-standard-program/overview-renewable-fuel-standard#compliance>. [Accessed: 24-Apr-2021].
- [58] J. R. Cruce and J. C. Quinn, “Economic viability of multiple algal biorefining pathways and the impact of public policies,” *Appl. Energy*, vol. 233–234, pp. 735–746, Jan. 2019.

APPENDIX A: SUPPLEMENTARY INFORMATION

Life Cycle Allocation Methods

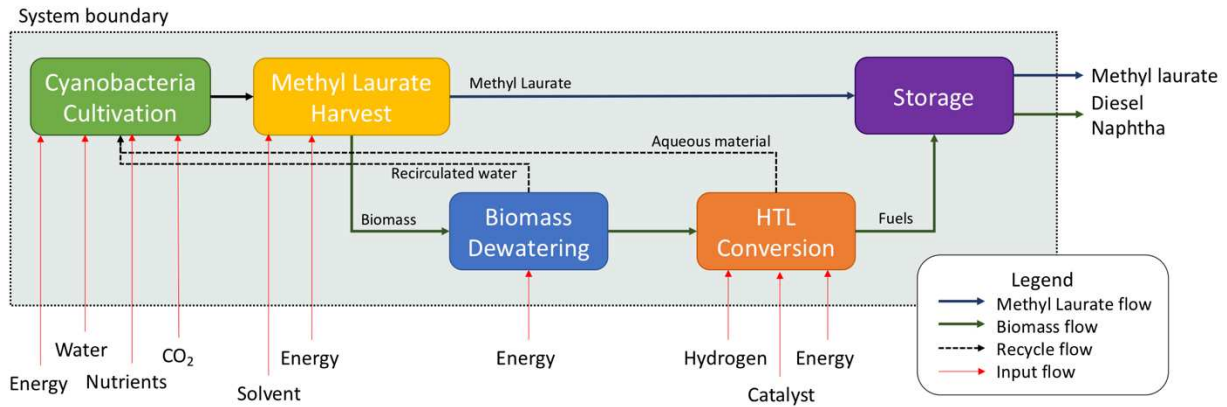


Figure A1: LCA allocation boundaries, where modules 100 (Cultivation), 200 (Harvest) and 500 (Storage) are allocated according to product economic value, and modules 300 (Dewater) and 400 (Conversion) are associated completely with the fuels.

Table A1: Results of mass and energetic allocation for 5th percentile, baseline, and 95th percentile scenarios.

	Mass allocation 5 th percentile – baseline – 95 th percentile	Economic allocation 5 th percentile – baseline – 95 th percentile
Portion of impacts allocated to fuels	51% – 63% – 71%	52% – 54% – 51%
Portion of impacts allocated to methyl laurate	49% – 38% – 29%	48% – 46% – 49%
Fuels GWP (g CO ₂ -eq/MJ)	94 – 115 – 161	93 – 115 – 148
Methyl Laurate GWP (g CO ₂ -eq/MJ)	-15 – 3 – 23	-14 – 3 – 38

Input Probability Distributions

Table A2: Probability distribution parameters for inputs related to overall process mass and energy.

Parameter (units)	Chosen Distribution	μ	Min	Max	Most Likely	Source	Notes
Pond productivity (g-m ⁻² day ⁻¹)	Uniform	13.5	12	15		[S1]	Pérez-López uses uniform for algal yield
Methyl laurate production ratio	Uniform	0.375	0.25	0.33		[S1]	Pérez-López uses uniform for biomass composition, which is analogous to secreted product
Mixer-settler energy requirement (kW-m ⁻³)	Uniform	0.07	0.04	0.1		[S2]	No information as to which value is more likely, only a range is given.
Dodecane concentration (L-L ⁻¹)	Uniform	0.001	0.0009	0.0011			FOAK uncertainty variable – vary by 10%
Flue gas purity	Uniform	98.5%	97%	100%		@RISK fitting tool, [S3]	Applied uniform distribution to range found in referenced source
CO ₂ utilization rate (%)	Triangular	33%	10%	40%	20%	[S1]	Pérez-López uses triangular for carbon sequestration but much lower, min of 0% max of 16%
Biocrude yield from HTL (%)	Triangular	40%	30%	60%	30%	@RISK fitting tool, [S4], [S5]	@Risk distribution fit to data found in literature, range directly matches Chen and Quinn 2021.
Operation days (days-yr ⁻¹)	Triangular	320	232	364	364	@RISK fitting tool, [S6]	Used @risk fitting tool on average productivity for the Southern US.

Table A3: Probability distribution parameters for economic inputs.

Parameter (units)	Chosen Distribution	μ	Min	Max	Most Likely	Source	Notes
Growth module CAPEX	Triangular	\$3.2M	\$1.8M	\$6.0M	\$1.8M	[S7]	Used @Risk to fit a distribution to pond CAPEX in Davis et al. 2016
Electricity cost (cts-kWh ⁻¹)	Triangular	6.73	6.39	7.01	6.79	[S1]	
Methyl laurate market value (\$-kg ⁻¹)	Triangular	\$1.78	\$0.85	\$3.00	\$1.50	[S8], [S9]	Abbas et al. methyl laurate and diesel prices from EIA are similar, used @Risk to fit a distribution to diesel prices from 2005 - 2020

Table A4: Probability distribution parameters for life cycle characterization inputs in kg-CO₂-eq-FU⁻¹.

Parameter (units)	Chosen Distribution	μ	Min	Max	σ	Shift	γ	β	α	Source	Notes
Hydrogen LCI (kg H ₂)	Uniform	10.9	12.9	8.9						[S10]	Cites the range 8.9 – 12.9 for hydrogen production, doesn't give probabilistic information
Electricity LCI (kWh)	Loglogistic						0.53	0.121	6	[S1]	Same underlying distributions as Pérez-López, different central values as determined from ecoinvent
Natural gas LCI (MJ)	Lognormal	0.01625			0.01625	0.15				[S1]	

Monte Carlo Analysis methodology

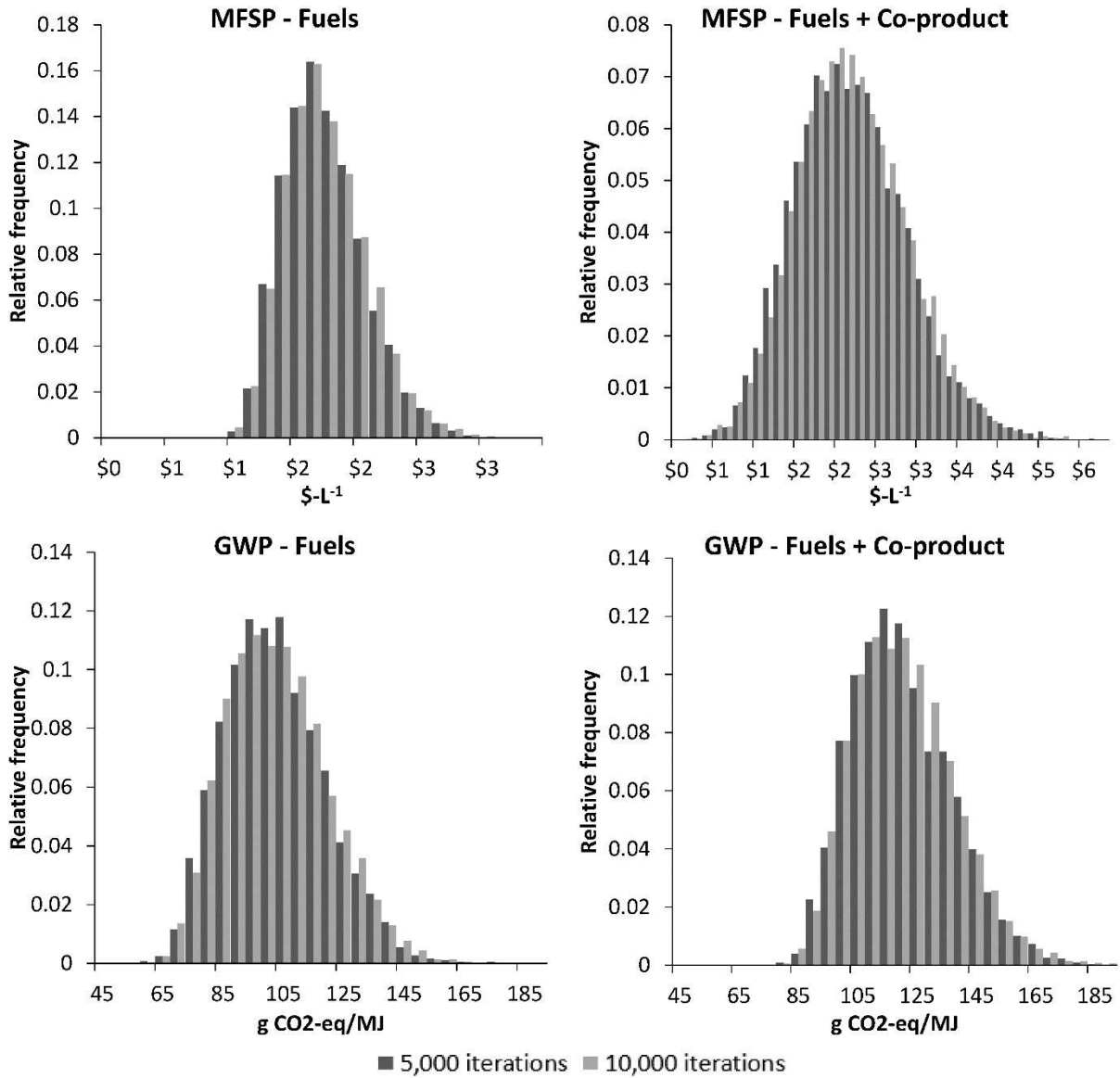


Figure A2: This dual histogram shows results for the MCA run with 5,000 iterations in dark grey and with 10,000 iterations in light grey. They have the same mean results and very similar spread and skew. This suggests that the chosen iteration number of 5,000 is sufficient.

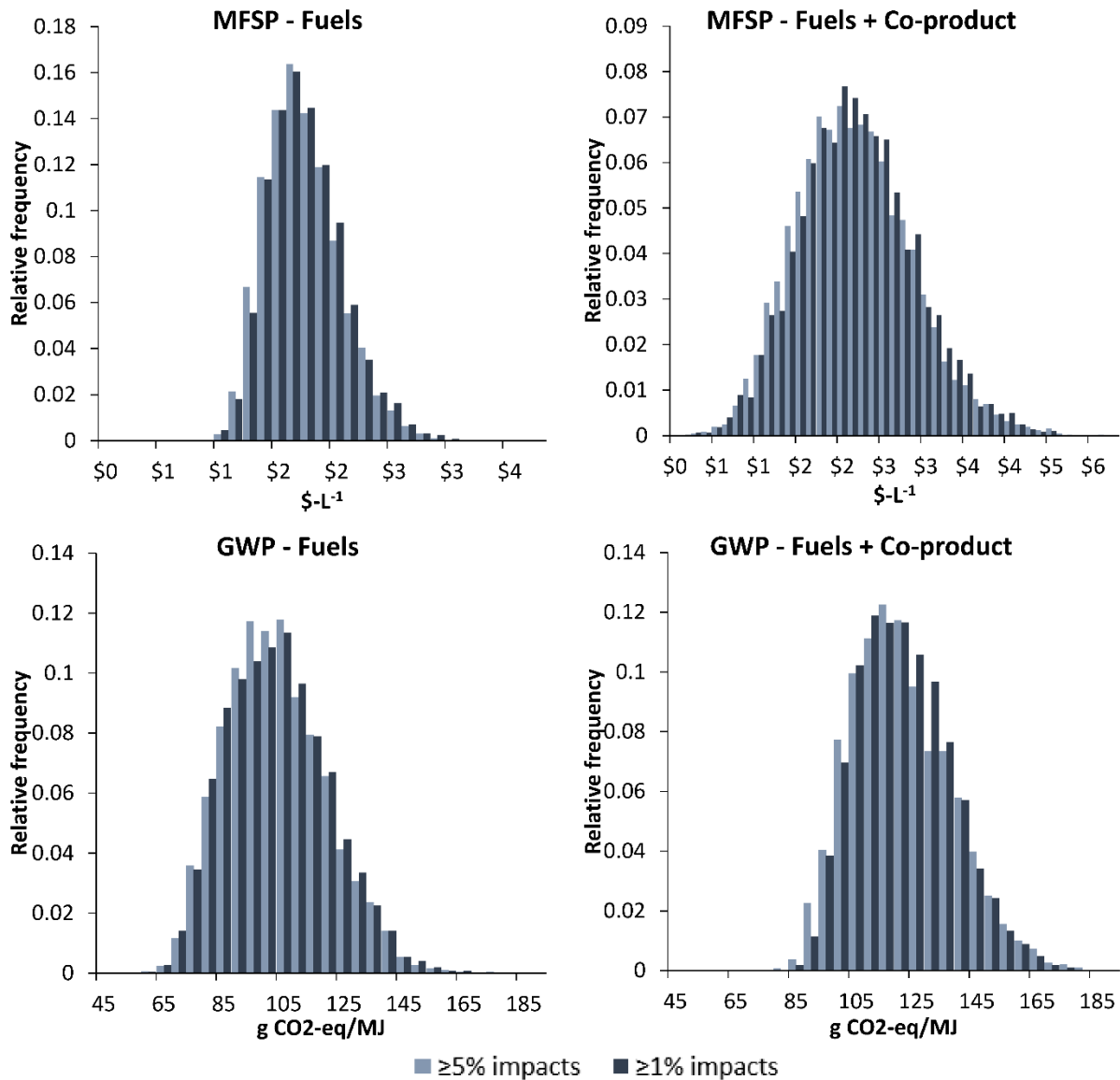


Figure A3: The dual histogram shows the MCA results for MFSP (top) and GWP (bottom) for the fuels case (left) and fuels + co-product case (right) for inclusion of parameters with at least 5% sensitivity impacts in light blue and 1% in dark blue. They have almost the same shape, with very similar mean results, standard deviation and skew. This suggests the choice to include parameters with at least 5% sensitivity impacts was sufficient.

Table A5: Summary statistics for the MCA results on TEA in $\$-L^{-1}$ for three combinations of MCA run parameters including selection criteria including 1% impacts and 10,000 iterations. These are compared to the presented results, which are generated by including parameters with 5% or greater sensitivity impact and an MCA run of 5,000 iterations.

	Parameter	≥5% impacts 5,000 iterations	≥5% impacts 10,000 iterations	≥1% impacts 5,000 iterations
Fuels	Mean	\$2.01	\$2.01	\$2.02
	Standard Deviation	\$0.34	\$0.34	\$0.34
	Skewness	0.5961	0.5779	0.5701
	5 th percentile	\$1.52	\$1.51	\$1.53
	95 th percentile	\$2.62	\$2.61	\$2.65
Fuels + co-product	Mean	\$2.47	\$2.47	\$2.50
	Standard Deviation	\$0.73	\$0.71	\$0.72
	Skewness	0.3854	0.5701	0.2898
	5 th percentile	\$1.35	\$1.38	\$1.36
	95 th percentile	\$3.74	\$3.70	\$3.77

Table A6: Summary statistics for the MCA results for three combinations of MCA run parameters including selection criteria including 1% impacts and 10,000 iterations. These are compared to the presented results, which are generated by including parameters with 5% or greater sensitivity impact and an MCA run of 5,000 iterations.

	Parameter	≥5% impacts 5,000 iterations	≥5% impacts 10,000 iterations	≥1% impacts 5,000 iterations
Fuels	Mean	100	100	100
	Standard Deviation	16.6	16.9	16.7
	Skewness	0.4166	0.4430	0.4227
	5 th percentile	75	75	73
	95 th percentile	130	130	173
Fuels + co-product	Mean	118	118	118
	Standard Deviation	17.0	17.0	15.6
	Skewness	0.5705	0.5862	0.4255
	5 th percentile	93	93	95
	95 th percentile	148	148	145

Supplementary Information References

- [A1] P. Pérez-López, M. Montazeri, G. Feijoo, M. T. Moreira, and M. J. Eckelman, “Integrating uncertainties to the combined environmental and economic assessment of algal biorefineries: A Monte Carlo approach,” *Sci. Total Environ.*, vol. 626, pp. 762–775, 2018.
- [A2] G. Towler and R. Sinnott, *Chemical Engineering and Design: Principles, Practice and Economics of Plant and Process Design*, 2nd ed. Waltham, MA: Butterworth-Heinemann, Elsevier Ltd., 2013.
- [A3] G. Last and M. Schmick, “Identification and Selection of Major Carbon Dioxide Stream Compositions,” no. June, p. 38, 2011.
- [A4] P. H. Chen and J. C. Quinn, “Microalgae to biofuels through hydrothermal liquefaction: Open-source techno-economic analysis and life cycle assessment,” *Appl. Energy*, vol. 289, no. February, p. 116613, 2021.
- [A5] Y. Hu, M. Gong, S. Feng, C. (Charles) Xu, and A. Bassi, “A review of recent developments of pre-treatment technologies and hydrothermal liquefaction of microalgae for bio-crude oil production,” *Renew. Sustain. Energy Rev.*, vol. 101, no. December 2018, pp. 476–492, 2019.
- [A6] J. M. Greene, D. Quiroz, S. Compton, P. J. Lammers, and J. C. Quinn, “A validated thermal and biological model for predicting algal productivity in large scale outdoor cultivation systems,” *Algal Res.*, vol. 54, no. January, p. 102224, 2021.
- [A7] R. Davis, J. Markham, C. Kinchin, N. Grundl, E. Tan, and D. Humbird, “Process Design and Economics for the Production of Algal Biomass: Algal Biomass Production in Open Pond Systems and Processing Through Dewatering for Downstream Conversion,” *Natl.*

Renew. Energy Lab., no. February, p. 128, 2016.

- [A8] S. K. Abbas, A. M. Belal, S. I. Bushrah, and W. Adeebah, “Production of 60,000 mtpa of oleochemical methyl ester from rbd palm kernel oil,” no. December 2015, 2016.
- [A9] U.S. Energy Information Administration, “EIA: Independent Statistics and Analysis: Petroleum and other liquids,” 2021. [Online]. Available: https://www.eia.gov/dnav/pet/hist/LeafHandler.ashx?n=PET&s=EMA_EPD2D_PWG_NUS_DPG&f=M. [Accessed: 03-Sep-2021].
- [A10] A. Mehmeti, A. Angelis-Dimakis, G. Arampatzis, S. J. McPhail, and S. Ulgiati, “Life cycle assessment and water footprint of hydrogen production methods: From conventional to emerging technologies,” *Environ. - MDPI*, vol. 5, no. 2, pp. 1–19, 2018.